CHALMERS
UNIVERSITY OF TECHNOLOGY

Early estimation of bridges with regards to LCA.

Parametric design study of three bridge types with regards to LCA

Master's thesis in Master Program Structural engineering and building technology

Pontus Rautio Pålsson
Andreas Svensson

Department of Architecture and Civil Engineering
CHALMERS UNIVERSITY OF TECHNOLOGY
Master's thesis ACEX30
Gothenburg, Sweden 2023

Master's thesis ACEX30-18-84

Early estimation of bridges with regards to LCA.

Parametric design study of three bridge types with regards to LCA

PONTUS RAUTIO PÅLSSON
ANDREAS SVENSSON

CHALMERS
UNIVERSITY OF TECHNOLOGY

Department of Architecture and Civil Engineering
Division of Building Technology
Concrete structures
Chalmers University of Technology
Gothenburg, Sweden 2023

Early estimation of bridges with regards to LCA
Parametric design study of three bridge types with regards to LCA

PONTUS RAUTIO PÅLSSON
ANDREAS SVENSSON

Examensarbete ACEX30
Institutionen för Arkitektur och Samhällsbyggnadsteknik
Chalmers tekniska högskola, 2023

Department of Architecture and Civil Engineering
Division of Building Technology
Concrete structures
Chalmers University of Technology
SE-412 96 Gothenburg
Telephone +46 (0)31 772 1000

Cover: The three bridge types investigated (Steel-concrete composite bridge, Slab bridge and Prestressed girder bridge).

Department of Architecture and Civil Engineering
Gothenburg, Sweden 2023

Early estimation of bridges with regards to LCA.
Parametric design study of three bridge types with regards to LCA
PONTUS RAUTIO PÅLSSON
ANDREAS SVENSSON
Department of Architecture and Civil Engineering
Division of Building Technology
Concrete structures
Chalmers University of Technology

Abstract

This study utilizes parametric design to determine cross-sections and quantifying materials, including their corresponding CO_2-equivalents, for single-span bridges, making it easy to identify the most suitable option from a LCA perspective. This is interesting because the Swedish construction sector accounts for a total of 21 % (Boverket, 2023) of the ecological footprint, which corresponds to 48 million tons of CO_2-equivalents.

Traditionally, experience-based dimensions are employed for efficient and rapid design according to our supervisors at Inhouse Tech AB. However, this compromises the bridge's full optimization regarding design loads and resistance, which is not ideal from a CO_2 perspective. As a result, this study has developed a programmed tool for each bridge type (deck slab-, prestressed girder-, and composite bridges). Where users simply input the width and length, and the output provides specific materials and their carbon footprints.

This study investigates specific carriageway widths of 6, 9, and 12 meters and every other meter for span lengths from 6 to 40 meters, to provide guidelines on which bridge type out of these three is most advantageous in terms of LCA.

The results show that slab bridges are more suitable for shorter spans when considering LCA. However, the choice of bridge type for longer spans varies and is highly dependent on the width of the carriageway.

Keywords: parametric, design-tool, LCA, optimization, bridges, prestressed, slab, steel-concrete, composite, MathCAD, early estimations.

Tidig uppskattning av broar med avseende på LCA.
Parametrisk designstudie av tre brotyper med avseende på LCA
PONTUS RAUTIO PÅLSSON
ANDREAS SVENSSON
Institutionen för Arkitektur och Samhällsbyggnad
Avdelningen för kontruktionsteknik
Betongbyggnad
Chalmers Tekniska Högskola

Sammanfattning

Denna studie använder parametrisk design för att bestämma tvärsnitt och kvantifiera material, inklusive deras motsvarande CO_2-ekvivalenter för enskilda brospann. Detta underlättar att identifiera det mest lämpliga alternativet ur ett LCA-perspektiv. Detta är intressant eftersom den svenska byggsektorn står för totalt 21 % (Boverket, 2023) av det ekologiska fotavtrycket, vilket motsvarar 48 miljoner ton CO_2-ekvivalenter.

Traditionellt används erfarenhetsbaserade dimensioner för effektiv och snabb design enligt våra handledare på Inhouse Tech AB. Men detta kompromissar brons fullständiga optimering med avseende på designlast och motståndskraft, vilket inte är optimalt ur ett CO_2-perspektiv. Som ett resultat har denna studie utvecklat ett programmerat verktyg för varje brotyp (plattbroar, förspända balkbroar och samverkansbroar). Användaren anger bredd och längd, och verktyget genererar specifika material och deras koldioxidavtryck som resultat.

Denna studie undersöker specifika bredder på körbanor med 6, 9 och 12 meter och varannan meter för spännvidder från 6 till 40 meter för att ge riktlinjer om vilken av dessa tre brotyper som är mest fördelaktig med avseende på LCA.

Resultaten visar att plattbroar är mer lämpliga för kortare spännvidder när man beaktar LCA. Dock varierar valet av brotyp för längre spännvidder och att detta är starkt beroende av körbanans bredd.

Nyckelord: parametrisk, designverktyg, LCA, optimering, broar, förspända, plattor, stål-betong, komposit, MathCAD, tidiga uppskattningar.

Contents

List of Figures

List of Tables

Acronyms

ALS Accidental limit state
EAF Electric arc furnace
EC Eurocode
EDP Environmental product declarations
FAT Fatigue limit state
FEM Finite element modelling
FLM3 Fatigue Load model 3
GWP Global warming potential
LBT Lateral torsional buckling
LCA Life cycle analysis
LM1 Load model 1
LM2 Load model 2
LM3 Load model 3
LM4 Load model 4
PCR Product category rules
SLS Serviceability limit state
ULS Ultimate limit state

Nomenclature

α	Adaption factor, Load model 1
αQi	Adaptation factor for concentrated loads, Load model 1
αqi	Adaptation factor for distributed load, Load model 1
α_{eff}	Effective modular ratio
β	Adaptation factor, Load model 2
χ_w	Reduction factor, web
$\Delta\sigma_C$	Responding fatigue resistance at 2 milion cycles for the
η	Material parameter
γ	Partial safety factor
γ_{Ff}	Partial safety factor for fatigue loading
$\gamma_{G,j,inf}$	Safety partial factor for favourable permanent loads
$\gamma_{G,j,sup}$	Safety partial factor for unfavourable permanent loads
$\gamma_{Q,1}$	Safety partial factor for unfavourable variable loads
$\gamma_{Q,i}$	Safety partial factor for favourable variable loads
λ_w	Slenderness, web
λ_1	Length of the span and structure type
λ_2	Taking the the traffic volume into account
λ_3	Time factor regarding the design life time of the bridge
λ_4	Taking the number of traffic lanes into account
λ_{max}	The maximum damage equivalent factor
ϕ	Diameter
Φ_2	Dynamic factor
$\Psi_{0,i}$	Combination factor
$\Psi_{1,i}$	Combination factor
$\Psi_{2,i}$	Combination factor
σ_{FLM}	Stress range due to the fatigue load model
ε	Dynamic contribution, Vehicle loads A-O
a_2	Placement of vertical stiffeners and transverse beams
c/c	Center to center distance
d	effective hegiht
f_{ctm}	Mean tensile strength
f_{yw}	Yield strength, web
$G_{k,j,inf}$	Characteristic, unfavourable permanent loads
$G_{k,j,sup}$	Characteristic, favourable permanent loads
h_w	Height, web
k_τ	Shear buckling coefficient
L	Total length of bridge

L_{el}	Support section length
L_{spv}	Span length of bridge
$M_{b.Rd}$	Moment design resistance
M_{Ed}	Moment design load
Q_{ak}	Concentrated load, Load model 2
Q_{ik}	Concentrated loads, Load model 1
q_{ik}	distributed load, Load Model 1
Q_{tk}	Centrifugal load
Q_v	Vertical concentrated loads
r	Radius
T_{Ed}	Torsional design load
$T_{Rd,max}$	Torsional design resistance
t_w	Thickness, web
$V_{bw.Rd}$	Design resistence web
V_{Ed}	Shear design load
$V_{Rd,max}$	Shear design resistance
w	total carriageway width
W_{el}	Elastic section modulus
w_I	notional lane

Preface

This Master's thesis is the culmination of the Master's program in Structural Engineering and Building Technology at Chalmers University of Technology. The research work was undertaken during the spring of 2023 at the bridge department of Inhouse Tech AB, located in Gothenburg.

We wish to express sincere gratitude to the supervisors at Inhouse Tech, namely Oscar Yman, Daniel Josefsson, and also Isak Wallo, for their invaluable support, guidance, and enthusiasm throughout the duration of this project. Their expertise and dedication significantly contributed to the successful completion of this thesis.

We would also like to extend appreciation to Joosef Leppänen, a Senior lecturer in concrete structures at Chalmers University of Technology, for serving as the examiner of this thesis. The guidance and feedback provided by Dr. Leppänen were instrumental in shaping the direction and quality of this research work.

Additionally, we would like to express gratitude to all the teachers involved in the courses undertaken during our academic journey. Their commitment and engagement in delivering quality education have played a vital role in shaping our knowledge and understanding.

1
Introduction

1.1 Background

There are different approaches to achieve the desired function and performance of a bridge structure. Material selection and material quantity (optimization) is strongly linked to function and performance, but also cost and the economic and environmental impact it entails. In a Swedish perspective, the construction industry is responsible for 21 % of the total carbon dioxide equivalent emissions, which corresponds to 48 million tonnes of carbon dioxide equivalents (CO_2-eq) (Boverket, 2023). A fraction coming from choice of material and material quantity. Preliminary designs of slab bridges and girder bridges are based on experience which may suggest oversized cross-sections that are retained throughout the whole design process if they meet the requirements according to the Eurocodes and the national annexes (Transportstyrelsen, 2018) (Trafikverket, 2022) (CEN., 2003) (CEN., 2002a) (CEN., 2002b) (Trafikverket, 2019). In this master thesis report, the task is to develop guidelines and recommendations in the early stages on which bridge type is most beneficial with regard to an Life Cycle Analysis (LCA) perspective. The task is developed in cooperation with Inhouse Tech AB, who indicates that the preliminary design of different bridge types leads to a conservative choice of cross sections in terms of material quantity and thus environmental impact.

1.2 Aim and objectives

The aim of this study is to use simple calculations to produce directives on which type of bridge has the least environmental impact from an LCA perspective using CO_2-eq/kg. Bridge types included in the study are.

- Deck slab bridge (reinforced concrete),
- Girder bridge (reinforced and prestressed concrete),
- Double girder steel-concrete composite bridge.

The goal in the project is to make early estimations of the environmental impact of simple supported bridges, and to reduce the amount of CO_2-equivalents.
The main objectives for this thesis are:

- Identify parameters in the design with large influence on the result for all investigated bridge types.

- Develop an optimization method for the studied bridges and compare them to each other to find the most optimal bridge type regarding environmental impact.

1.3 Limitations

To simplify and make the bridges comparable, the study has been limited. The bridges being investigated are single span bridges of the types: slab bridges, girder bridges and steel-concrete composite girder bridges where the superstructure is of main interest. The bridges have the same prerequisites for the geometry of end shields, wing walls which are a function of the horizontal displacement caused by temperature load, braking and overload (Trafikverket, 2022). In addition to this, the load cases have been limited to those that make up the majority of the load effect, namely variable loads such as traffic loads, permanent loads such as self-weight and earth pressure which together produce load effects such as moment, shear force and normal force.

- Single span bridges with end shields
- Geotechnical aspects are not considered.
- Only the superstructure will be considered.
- Road traffic action (not rail traffic action)
- The bridge is assumed to be straight with no radius.

2

Design of simply supported end shield bridges

The following chapter covers the theory of simply supported bridges and the structural parts for each bridge type. The chapter continues by describing load actions on a bridge structure and how they are combined in the design process with load combinations. Environmental impact from construction buildings is investigated and the theory behind the calculation model for LCA is presented.

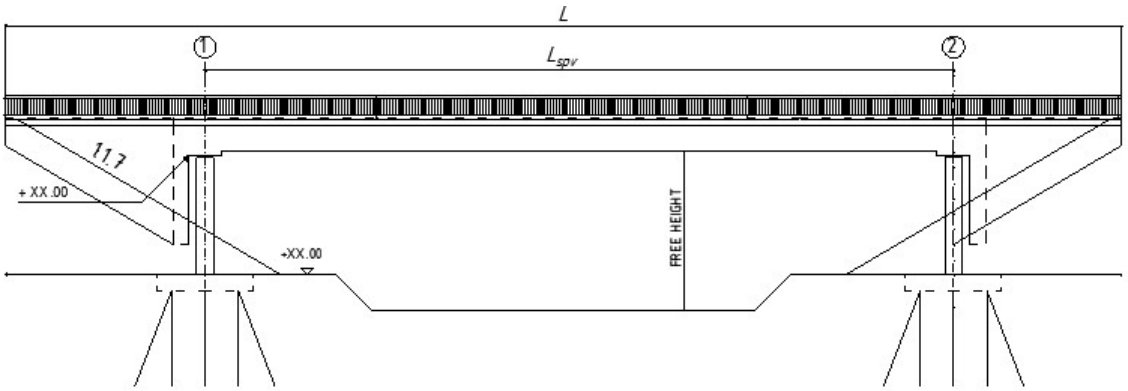

Figure 2.1: *Slab bridge.*

2.1 Slab bridge

Slab bridges are a good choice when the construction height is limited. Available construction height is approximately 6 % of the span. This bridge type is considered effective up to spans of 20-25 meter. In a slab bridge, the superstructure consists of a homogeneous concrete slab, simply supported on the end supports. The following condition needs to be fulfilled to define the bridge as a slab bridge according to (Trafikverket, 2008):

- The superstructure consists of one element with a width five times larger than the height of the slab. ($B > 5 \cdot H$).
- Longitudinal reinforcement is uniformly distributed along the width of the slab.

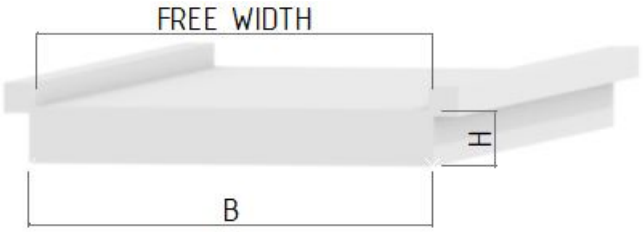

Figure 2.2: *Section slab element.*

2.1.1 Girder bridge

The girder bridge is carried out in one or more spans where the main supporting structure is usually designed with one or more beams. The girders are usually designed of steel, wood, or concrete with slack reinforcement or prestressed reinforcement. This study focuses only on reinforced and prestressed concrete.

The span length varies depending on the choice of material and reinforcement method. Concrete girder beams with slack reinforcement are usually designed up to 25 meter and with prestressed reinforcement span lengths up to 200 meter can be achieved. Prestressed reinforcement can be a decisive factor at 20-25 meter spans where construction height is limited (Trafikverket, 2008).

To define a bridge as a girder bridge, the following criteria need to be met according to (Trafikverket, 2008) :

- Its main supporting structure consists of one or more girders where the beams have a width that is less than or equal to five times the height ($B \leq 5 \cdot H$).
- In concrete girder bridge the longitudinal reinforcement at the top is usually concentrated within or next to the girder width B.

The increase of girders in a girder bridge does not necessarily decrease each girders traffic action load impact due to the load distribution is mainly carried in the longitudinal direction, therefore it's appropriate to minimize the number of girders. In cases with wide and heavily trafficked bridges, it might be effective to increase the number of girders with regard to maintenance (Vägverket, 1996). When designing a girder bridge the distance between the girders needs to be decided, according (Vägverket, 1996) following guidelines should be followed:

- The bridge deck cantilever is approximately 40 % of the girder's c/c distance.
- The bridge deck cantilever is usually less than 2.5 meters.

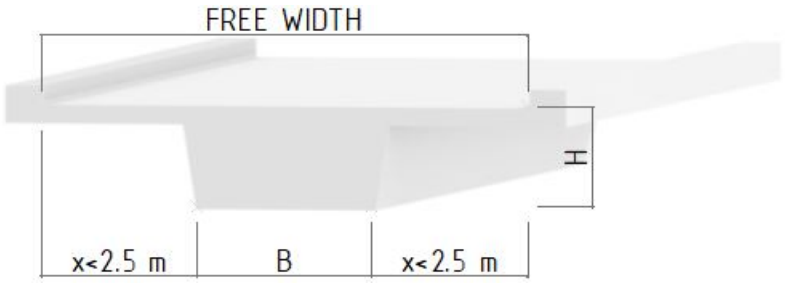

Figure 2.3: *Section girder bridge element.*

2.1.2 Steel-concrete composite girder bridge

Composite bridges are usually designed with steel girders and concrete bridge deck slabs and are connected with welded bolts in the upper flange to transfer the loads see Figures 2.4 - 2.5. In a composite bridge, the high tensile strength of the steel is utilized at the same time as the high compressive strength of concrete is utilized. The span length for composite bridges is usually in the range of 20-70 meter, and a practical limitation is steel web height compared to the steel mill's maximum rolling width (Vägverket, 1996).

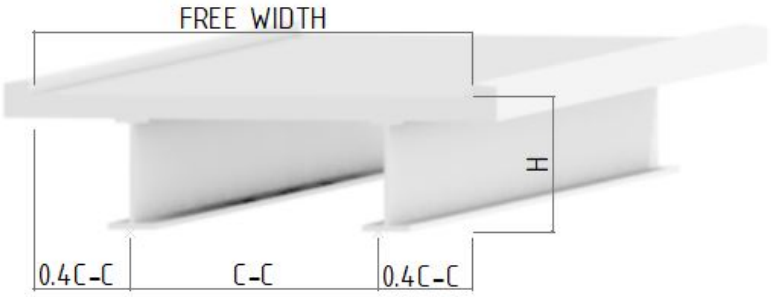

Figure 2.4: *Section composite bridge element(s).*

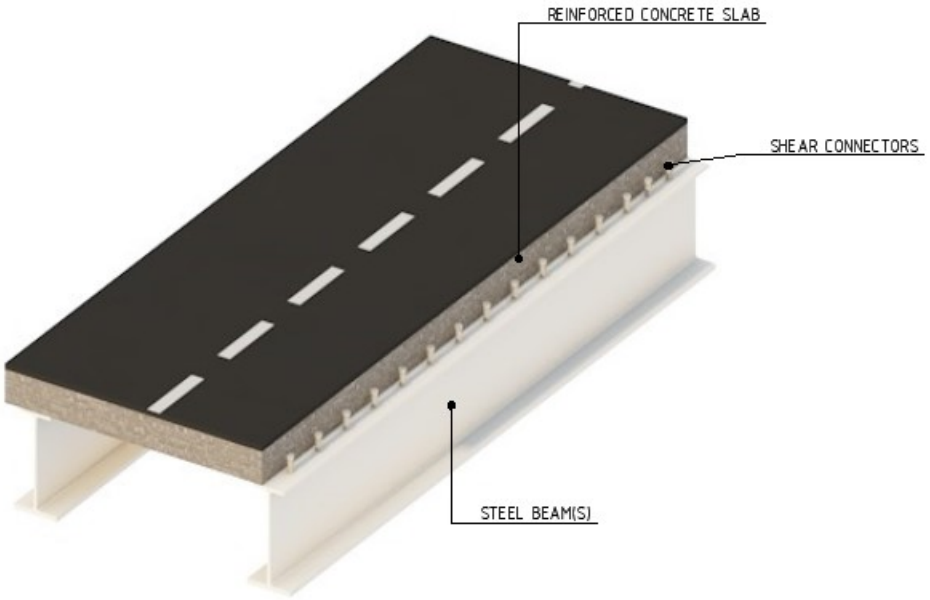

Figure 2.5: *Steel-concrete composite girder bridge.*

2.1.3 Bridge with end shield

In this thesis three different bridge types were investigated and one common construction detail for them is that they will have elevated foundations at end abutments with end shields. End supports are constructed on an elevated foundation either as piles or plates depending on the magnitude of the load and ground conditions. To prevent horizontal forces from the earth pressure on the footing foundations a end shield is constructed with wing walls, and the backfill soils interaction with the end shield provides stabilization for the superstructure (Vägverket, 1996).

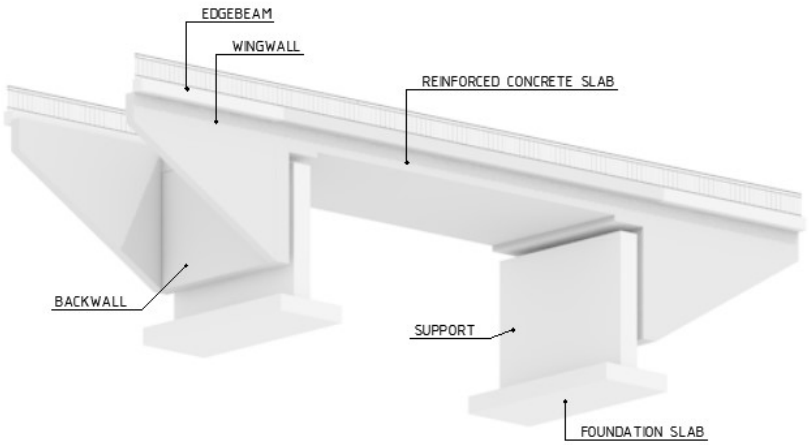

Figure 2.6: *Reinforced concrete slab with end shield.*

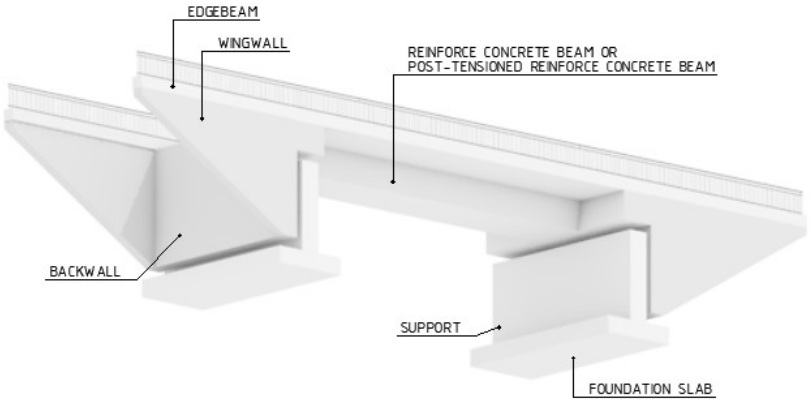

Figure 2.7: *Girder bridge with end shield.*

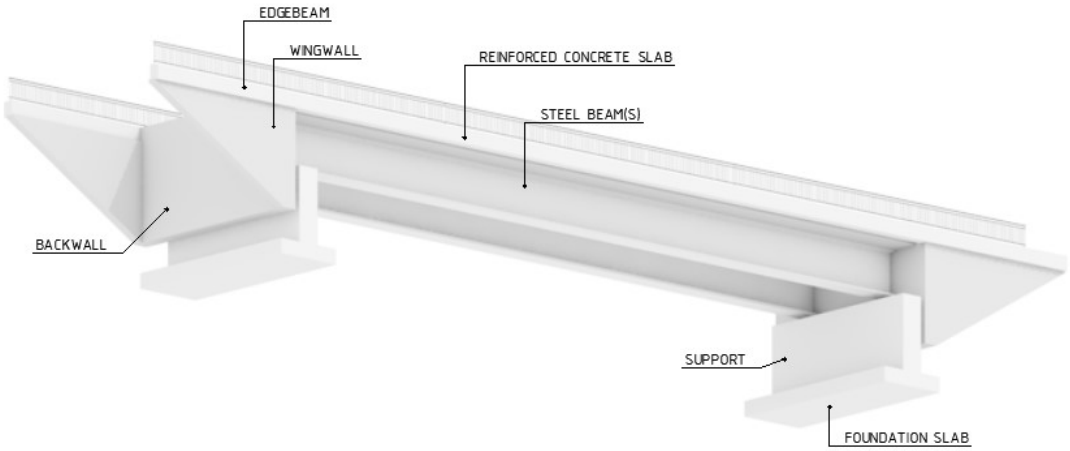

Figure 2.8: *Steel-concrete composite bridge.*

2.2 Design method

This chapter describes load actions on a structure, based on the Eurocodes (CEN., 2002a) (CEN., 2002b). EN-1990 describes basics of structural safety, serviceability, and durability and EN-1991 describes actions on structures. Together with the national annex for vehicle loads (Transportstyrelsen, 2018), these give a directive on how to treat the affecting load actions on a bridge structure as a basis for structural design in Serviceability Limit State (SLS) and Ultimate Limit State (ULS).

Actions can either work as direct or indirect. Eurocodes defines direct loads as "Set of forces (loads) that is applied directly to the structure" and indirect actions as "Set of imposed deformations or accelerations caused for example by temperature changes, moisture variations, uneven settlements or earthquakes". These actions give rise to an effect in structural members such as internal forces, moments, stresses, strains, deflection and rotation on an entire structure (CEN., 2002a).

The origin of the load also determines whether the direct load is fixed or free to move. The load action is in the Eurocode categorized by the situation/the variation in time of the load effect. These situations are defined as Permanent load **(G)**, Variable load **(Q)** and Accidental load **(A)**.

Permanent loads include loads that affect the structure or structural part during normal use. A permanent load generally has a reference period of the entire lifetime of the structure. Permanent loads include, for example, self-weight of structural and non-structural elements.

Variable loads is present at a frequency or interval unlike permanent loads. These include, for example, traffic loads on bridges and wind loads. Reference period for climate loads such as wind and snow loads generally has a reference period of one year.

Accidental loads arise in exceptional cases, for example in the event of a fire, earthquakes or other accidental loads. There are several parameters that define an accident load. The reference period is usually short, it occurs at one time and is of short duration. Although the probability of its occurrence during the life of the structure is low, it must be taken into account because the consequence might be of a catastrophic nature.

2.2.1 Load actions on bridges

- **Permanent load (G)**: Self-weight, earth pressure, shrinkage, creep.
- **Variable load (Q)**: wind loads, traffic loads, thermal loads, horizontal variable load, acceleration and braking, centrifugal load, surcharge load, transverse horizontal load.
- **Accidental load (A)**: inoperative tendon and collision with railings etc.

2.2.1.1 Self-weight

Self-weight can be, for example, reinforced concrete, paving and railings. It is regulated both in the Eurocodes in (CEN., 2002b) and in the Swedish Traffic Agency's (Trafikverket, 2022) regulations for infrastructure.

2.2.1.2 Earth pressure

Earth pressure can act both horizontally and vertically against the bridge structure. Depending on how the earth pressure acts or does not act against the bridge, it can be active, passive or earth pressure at rest.

2.2.1.3 Shrinkage

The total shrinkage can be divided into drying shrinkage and autogenous shrinkage. Drying shrinkage is with the exchange of moisture (moisture transport) between a concrete structure and the surrounding air during long time. Moisture transport is driven by different levels of relative humidity in the concrete and surroundings. It is therefore very dependent on elements parts exposed to the surrounding air. Drying shrinkage is a function of time and permeability (the concrete's ability to release moisture), the relative humidity of the environment, exposure to the environment and the concrete class.

Autogenous shrinkage is a type of chemical reaction that takes place in the hydration process, i.e., when the cement reacts with the water. This is called autogenous shrinkage and is distinct from drying shrinkage and is not dependent on ambient moisture, but on the amount of water mixed into the cement. Autogenous shrinkage is a function of time and the strength class of concrete (Engström, 2007).

2.2.1.4 Creep

Creep is an effect that is highly dependent on time, stress and moisture transport (and ambient humidity). This is calculated as an contributing elastic strain when loaded at time (t). A concrete that is subjected to load before fully developed strength (28 days according to the Eurocodes) is, for example, very sensitive to stresses compared to older concrete. There are different ways to calculate the creep, but the most accurate, with the possibility to consider the loading history, is the superposition method (Engström, 2007).

2.2.1.5 Wind load

The wind load is a horizontal load that affects the bridge. The wind load is acting both on the bridge itself and also the on vehicles on it. The wind load is calculated using the reference velocity pressure, which is an average velocity value of the last 50 years for a certain region.

2.2.1.6 Traffic loads

A traffic load is free to move in the direction of the carriageway, but is considered as a static load for every possible load case along the entire span length of the bridge.

Traffic loads are regulated both in the Eurocodes (CEN., 2003) and in the national annex A-O Vehicle loads (Transportstyrelsen, 2018). In the Eurocodes, a load model is presented to cover both trucks, cars, and pedestrians in global and local calculations.

The total carriageway width (w) is defined by the number of notional lanes and the remaining width (CEN., 2003). Thus, EC assumes limitation of loads distribution within the notional lane (w_I). The notional lane width is 3 meter except for special cases with two notional lanes without any remaining width (5.4 m $\leq w <$ 6 m).

Carriageway width w	**Number of notional lanes**	**Width of a notional lane** w_l	**Width of the remaining area**
$w < 5{,}4$ m	$n_1 = 1$	3 m	w - 3 m
5,4 m $\leq w <$ 6 m	$n_1 = 2$	$\frac{w}{2}$	0
6 m $\leq w$	$n_1 = Int\left(\frac{w}{3}\right)$	3 m	$w - 3 \times n_1$
NOTE For example, for a carriageway width equal to 11m, $n_1 = Int\left(\frac{w}{3}\right) = 3$, and the width of the remaining area is 11 - 3×3 = 2m.			

Figure 2.9: *Notional lane width, from (CEN., 2003).*

The numbering of the load cases must correspond to Figure 2.10. The most unfavourable load is placed in load lane 1 and then increases in numerical order while the unfavourable effect decreases, with the least unfavourable effect in load lane 3. The placement of the load fields does not necessarily have to agree with the figure.

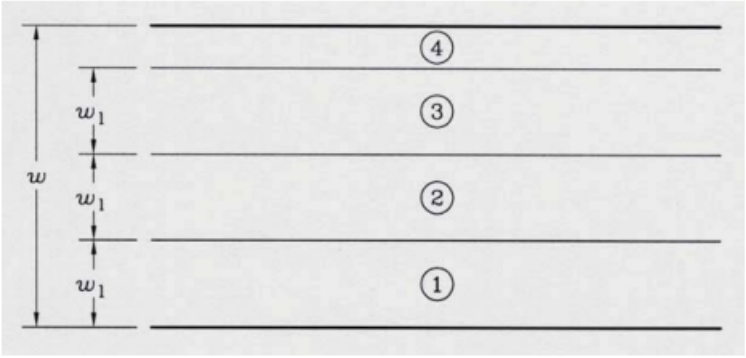

Key
w Carriageway width
w_1 Notional lane width
1 Notional Lane Nr. 1
2 Notional Lane Nr. 2
3 Notional Lane Nr. 3
4 Remaining area

Figure 2.10: *Notional lane numbering, from (CEN., 2003).*

In EC, traffic loads are regulated by four different load models. In this thesis, Load Model 1 (LM1) and Load Model 2 (LM2) and is used for calculations. Special vehicles are treated in model 3 (LM3) is therefore excluded. Load model 4 (LM4) is excludes as this is intended for public gatherings and thus will not be decisive.

Load model 1 (LM1)
LM1 is divided into distributed loads (q_{ik}) and two point loads (Q_{ik}). The point loads represent a bogie system (double axles) of a vehicle, that covers both trucks and cars. The distributed load represents pedestrians. The point load is multiplied by a factor α and thus the load becomes αQi and distributed load is multiplied by the same factor and thus the distributed load becomes αqi, which is presented in the national annex (Transportstyrelsen, 2018). A load multiplied by this reduction factor corresponds to a traffic class. In calculations where the contact area and wheel distribution for an axle is needed, this is the same as in LM2. The dynamic contribution from vehicles is included in LM1.

The magnitude of the worst case, load lane number 1: where Q_{1k} is 300 kN and the distributed load q_{1k} 9 kN/m^2 in LM1 see Figure 2.11.

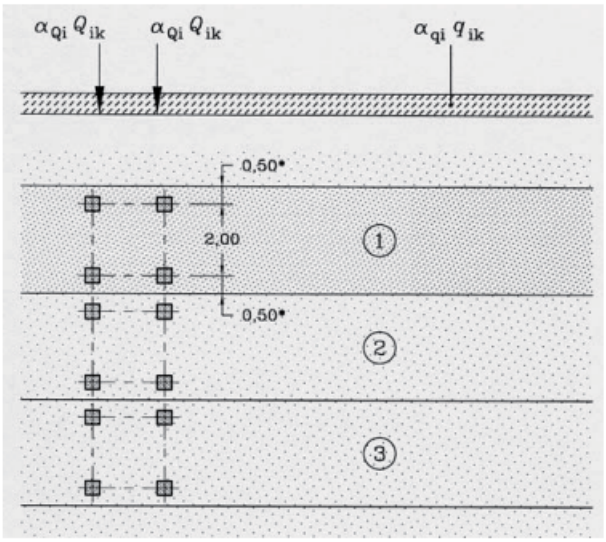

Key
(1) Lane Nr. 1 : $Q_{1k} = 300$ kN ; $q_{1k} = 9$ kN/m^2
(2) Lane Nr. 2 : $Q_{2k} = 200$ kN ; $q_{2k} = 2{,}5$ kN/m^2
(3) Lane Nr. 3 : $Q_{3k} = 100$ kN ; $q_{3k} = 2{,}5$ kN/m^2
* For $w_l = 3{,}00$ m

Figure 2.11: *Numbering and loads, from (CEN., 2003).*

Load model 2

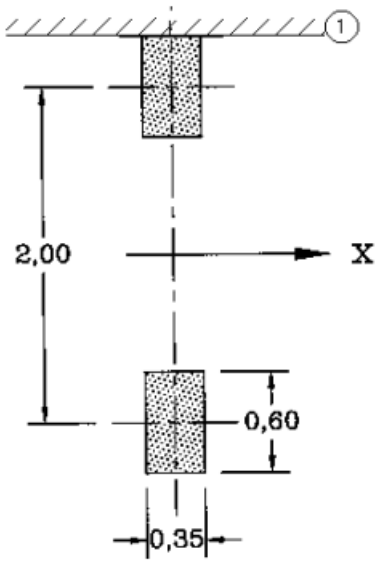

Key
X Bridge longitudinal axis direction
1 Kerb

Figure 2.12: *Numbering and loads, from (CEN., 2003).*

LM2 consists of a point load (Q_{ak}). The point load represents an axle (half a boogie system) of a vehicle with specific areas where the wheels are located. The point

load is multiplied with the factor β and the load becomes βQi , which corresponds to the Q_1 as the factor is set to 0.9 (Transportstyrelsen, 2018). Dynamic effects are included in LM2.

A-O Vehicle loads
Traffic loads in the national annex (Transportstyrelsen, 2018) describes the typical Swedish vehicle loads and their various combinations that can conceivably cross a bridge. There are currently fifteen different combinations that are named in alphabetical order from A to O. Axle loads and boogie systems are described as point loads similar to LM1 while distribute loads are described as kN/m.

An example is shown below on vehicle model I from typical loads. The distributed load can be either 0 or 5 kN/m, depending on which case is most unfavourable. The point loads are described as fractions of the axle load A = 180 kN and B = 300 kN. in the case of typical vehicle load I shown below, only fractions of B are used.

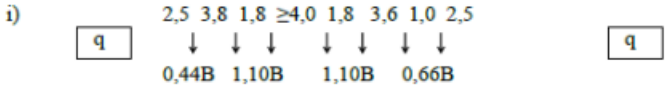

Figure 2.13: *Vehicle load I, from (Transportstyrelsen, 2018).*

The dynamic contribution is not included in vehicle loads A-O. It is calculated as a percentage increase of the vertical point loads included in the specific model. This contribution is described as ε and should be 25 % (Trafikverket, 2022). With exception of the ground fill and paving together exceeding a height of 0.3 m. Then it can be interpolated between 0 % and 20 %, where 0.3 m corresponds to 25 % dynamic addition of the point loads and 0 % corresponds to a height of 0.5 m. Anything over 0.5 m and above does not need a dynamic contribution.

2.2.1.7 Acceleration and braking

Acceleration and brake loads in longitudinal direction are horizontal loads that occur when vehicles accelerate or brakes that works. In EC (CEN., 2003) the load vector for both acceleration and braking is equal in magnitude but in opposite longitudinal direction. The horizontal load is placed at the contact surface between the tire and the road surface, i.e., on top of the pavement.

Acceleration and braking loads must be calculated for the most unfavourable case between load models in the Eurocodes and the type vehicles A-O described in the national annex (Transportstyrelsen, 2018).

In LM1, these loads are calculated as fractions of the vertical of the axle loads and fractions of the total load on the road surface as in Equation 2.1.

$$Q_{1k} = 0.6_{\alpha Q1}(2Q_{1k}) + 0.10_{\alpha q1} q_{1k} w_1 L \tag{2.1}$$

$$180_{\alpha Q1} kN \leq Q_{1k} \leq 900kN \tag{2.2}$$

In type A-O vehicles, the acceleration and brake load is set to 35 % of the total vertical load (without the dynamic contribution), however it must not exceed 500 kN (Transportstyrelsen, 2018).

2.2.1.8 Centrifugal load

The centrifugal load acts in the direction of the radius at the level of the paving with a bridge radius in meters (r), which can be determined with the curvature of the edge beam. The same calculation model is used for both the national annex and the Eurocode model LM1 for centrifugal load, as a function of the radius and vertical point loads (without the dynamic contribution) (CEN., 2003). The most unfavourable vertical load case is used in calculations.

$Q_{tk} = 0{,}2Q_v$ (kN)	if $r < 200$ m
$Q_{tk} = 40Q_v / r$ (kN)	if $200 \leq r \leq 1500$ m
$Q_{tk} = 0$	if $r > 1500$ m

Figure 2.14: *Centrifugal load, from (CEN., 2003).*

2.2.1.9 Thermal loads

The temperature effect is referred to young concrete which in the hydration process creates a reaction and heat increase and cooling before and when the concrete's strength properties develop. Initially, the temperature increases and expands as a function of cement temperature, cement type and volume, reaching its highest temperature. The increase in temperature is followed by a cooling process where the concrete need time to contract. If the concrete is not free to move due to the degree of external restraint or internal restraint, there is a risk of cracks occurring, which in this way inhibits durability (Engström, 2007).

2.2.1.10 Surcharge load

Surcharge loads can be derived from vertical loads from vehicles adjacent to the bridge on the carriageway. Combined with vertical load action from the soil, these creates a lateral earth pressure against end shields and wing walls.

2.2.1.11 Increased earth pressure

Horizontal loads along the bridge such as temperature load, brake load, acceleration load and surcharge are taken up by the end shields and need to be counted as a contribution to the earth pressure.

2.2.1.12 Transverse horizontal load

Transverse horizontal loads arise on top of pavement on the carriageway. These originate from vehicles skew braking or skidding. These are calculated as fractions

(25 %) from longitudinal braking or acceleration force in load model 1 (CEN., 2003). The same method applied when A-O vehicle load is the most unfavorable load case according to Transportstyrelsen, 2018.

2.2.1.13 Reduced prestress area

Inoperative tendon cable is means that the moment capacity is reduced through loss of prestress reinforcement area corresponding to one tendon cable. This is done in case one of the tendons is not working properly. This accidental load case is regulated by (CEN., 2003), (Trafikverket, 2019) and (Trafikverket, 2022).

2.2.1.14 Collision with pedestrian railing

Hitting the bridge railing is an accidental load that can occur when vehicles, for example, accidentally drive into the railing. These are regulated in (CEN., 2016) with additions from (Trafikverket, 2022).

2.2.2 Load combinations

Limit states are divided into Ultimate Limit State (ULS) and Serviceability Limit State (SLS). ULS is defined as collapse or some other form of failure, while SLS is not associated with collapse, but the comfort for users or the appearance during normal use. A load combination in these sates include both permanent load (**G**) and variable load (**Q**). Fatigue limit state (FAT) considers material which exposed to cyclic loading where fatigue can be decisive. Accidental limit state (ALS) is used for a construction or a member that is to be designed for a specific accidental event, that might have catastrophic outcome.

2.2.2.1 Ultimate Limit State (ULS)

Depending on which verification is to be carried out in the **Ultimate Limit State**, a specific load combination and a set of partial factors are used. There are three sets of partial factors A-C referring to tables A1.2(A-C) (CEN., 2002a p. 48). The load combinations are known as **EQU, STR, GEO** and will be further described below.

EQU:
If a verification is to be done for lost static equilibrium of a structure, **EQU** load combinations is used as in Equation 2.3. Set A of partial factors is combined with permanent and variable load.

$$\sum_{j\geq 1} \gamma_{G,j,sup} G_{k,j,sup} \text{"} + \text{"} \gamma_{G,j,inf} G_{k,j,inf} \text{"} + \text{"} \gamma_{Q,1} Q_{k,1} \text{"} + \text{"} \sum_{i\geq 1} \gamma_{Q,i} \Psi_{0,i} Q_{k,i} \tag{2.3}$$

STR and GEO:
Verification of a structure or structural member where the possibility of internal failure which is depending on the material strength, **STR** load combinations is used.

The same pair of equations holds for geotechnincal actions considering failure of soil masses resulting in large deformations of the foundation, known as **GEO** load combination.

STR and GEO are divided into Equations 2.4 and 2.5. The most unfavorable of these should be used for the specific verification. For **STR** partial factors from set B is used for both geotechnical and other loads (Trafikverket, 2019). For **GEO** set of partial factors according to set B must be applied for all traffic loads except traffic load on the connecting bank if the bridge is equipped with overfill or ballast, but partial factors according to set C for geotechnical loads (Trafikverket, 2019).

The permanent loads are divided into *favourable* permanent loads and *unfavourable* ones respectively. The variable loads are divided into *leading variable action* and *accompanying variable actions*, with the latter one subdevided into *main actions* or *other actions*.

Partial safety factor γ for permanent and variable load is chosen as the recommendations according to Eurocodes and thenational annex. ξ is a reduction factor for unfavourable permanent load ($G_{k,j,sup}$) and Ψ is a combination factor given in the national annex. Partial safety γ_d corresponds to a safety class from 1-4 with different scaling (Table 2.1). For road bridges with a theoretical span of no more than 15 m, safety class 2 should be applied. For span lengths over 15 m, safety class 3 should be applied according to Trafikverket (Transportstyrelsen, 2018).

Table 2.1: Safety classes.

Safety class	γ_d
1	0.83
2	0.91
3	1.0
4	1.1

$$\sum_{j\geq 1} \gamma_{G,j,sup} G_{k,j,sup}" + "\gamma_{G,j,inf} G_{k,j,inf}" + "\gamma_{Q,1}\Psi_{0,1} Q_{k,1}" + "\sum_{i\geq 1} \gamma_{Q,i}\Psi_{0,i} Q_{k,i} \quad (2.4)$$

$$\sum_{j\geq 1} \xi_{G,j,sup}\gamma_{G,j,sup} G_{k,j,sup}" + "\gamma_{G,j,inf} G_{k,j,inf}" + "\gamma_{Q,1} Q_{k,1}" + "\sum_{i\geq 1} \gamma_{Q,i}\Psi_{0,i} Q_{k,i} \quad (2.5)$$

2.2.2.2 Serviceability Limit State (SLS)

Depending on which verification is to be carried out in the **Serviceabilty Limit State**, Characteristic-, Frequent- or Quasi-permanent combination can be applied.

Characteristic combination is defined by irreversible limit states, as in Equation 2.6.

$$\sum_{j\geq 1} G_{k,j,sup}" + "G_{k,j,inf}" + "Q_{k,1}" + "\sum_{i\geq 1} \Psi_{0,i} Q_{k,i} \quad (2.6)$$

Frequent combination is defined by reversible limit states, as in Equation 2.7.

$$\sum_{j\geq 1} G_{k,j,sup}" + "G_{k,j,inf}" + "\Psi_{1,1}Q_{k,1}" + "\sum_{i\geq 1} \Psi_{2,i}Q_{k,i} \tag{2.7}$$

The Quasi-permanent combination is defined by long term effect, as in Equation 2.8. In this load combination, combination factor Ψ_2 shall be applied for an increased earth pressure caused by temperature change according to (Trafikverket, 2019).

$$\sum_{j\geq 1} G_{k,j,sup}" + "G_{k,j,inf}" + "\sum_{i\geq 1} \Psi_{2,i}Q_{k,i} \tag{2.8}$$

Deflection caused by variable load on road bridges shall not exceed $L_{spv}/400$ and the deflection or horizontal deformation shall not exceed $L_{spv}/200$ where L_{spv} corresponds to the theoretical span length. (Trafikverket, 2019). The deflection of the cantilever needs to be checked in SLS with frequent combination, and according to (Trafikverket, 2022) it should be limited to 5 mm.

2.3 Life Cycle Analys (LCA)

The building and construction sector in Sweden aims to reach net zero emissions of greenhouse gases 2045 (Fossilfritt Sverige, 2018). In 2020 the building and construction sector in Sweden accounted for 21 % of the total carbon dioxide equivalents emissions (Boverket, 2023). In order to reach the goals, the entire sector, from material production to recycling work, needs to change. In order to get a measure of how the construction affects the environment, a calculation tool called life cycle analysis has been developed and the basics are presented in this chapter.

LCA is a method for calculating the environmental impact of a product's entire life cycle, from extracting the raw material until the product has been consumed or recycled. With an LCA of constructions the output gives at which stage of a construction life cycle a certain environmental impact is greatest, with the results the design can be optimized with less environmental impact.

An LCA aims at an overall assessment of the environmental impact. The results include various categories of environmental impact, the LCA standards for construction applied in Europe currently include the following environmental impact categories according to (Boverket, 2019b):

- Climate impact greenhouse gases (GWP- Global warming potential)
- Acidification (AP- Acidification potential)
- Eutrophication potential (EP- Eutrophication potential)
- Depletion of non-fossil resources (ADPe - Abiotic depletion potential elements)
- Depletion of fossil resources (ADPf- Abiotic depletion potential fossil fuels)
- Ozone depletion (ODP- Ozone depletion potential)
- Ground level ozone (POCP- Photochemical oxidant creation potential)

2.3.1 LCA bridge design

The designer has an important part in ensuring that the construction has a low climate footprint. The designer can work early in the design process to optimize the construction and choose a resource-efficient construction to reduce carbon dioxide emissions according to (Svensk Betong, 2022).

2.4 Environmental impact of concrete and steel structures

In this study, the carbon dioxide emissions from the materials will be evaluated to compare the material to each other, the global warming potential (GWP) is defined for each material and then multiplied by the volume that is used for the construction. GWP for each material can be found in product-specific declarations called environmental product declarations (EPD) where the product's environmental impact is declared by an LCA. When comparing the GWP for different materials it must be done by the same product category rules (PCR) according to (Boverket, 2019a).

2.4.1 Concrete

Concrete is made of crushed stone material, water, binder, and small amounts of additives.The largest influence on the climate impact regarding manufacturing comes from the production of clinker which is the main component of cement and is made from heated limestone. According to (Svensk Betong, 2022) it can be proved with high reliability that clinker production stands for 90 % of the total carbon emissions from concrete calculated with LCA methodology, the remaining part comes from transport, other component materials, and production processes.

2.4.2 Steel

The production of structural steel leads to both direct and indirect emissions of carbon dioxide. Direct emissions mainly occur during production when iron oxide is fused with carbon. Indirect emissions occur during the manufacturing and delivery of raw materials together with the transportation to the customers (Jernkontoret, 2018). The production method for reinforcement steel is different as there are not as high demands on the final product of construction steel, therefore scrap metal can be used with the production method called electric arc furnace (EAF) to produce reinforcement steel with less GWP. CO_2-equivalents for structural steel, reinforcement steel, and concrete are presented in Table 2.2 and are taken from (Tyrens, 2019).

Table 2.2: CO_2-eq for construction materials.

Type	CO_2**-eq**	**Unit**
Reinforcement steel	6019	kg/m^3
Prestressing reinforcement	9458	kg/m^3
Structural steel	18916	kg/m^3
Concrete	467	kg/m^3

3
Optimization methods

In order to carry out the optimization of all three bridge types, specific limitation, simplifications and estimations are made concerning load effects and the preliminary sizing of the superstructure. Some parts of these limitations are not based on the Eurocodes, but instead on "buildability", which is considered realistic and feasible in the industry. This will be presented under each bridge types subchapter.

All three bridges have in common that the geometry of the wing walls and end shields are based on the horizontal displacement at the end of the bridge. This geometry is a function of the span length, temperature changes, braking and overload, which results in a design that is the same for all three bridge types with the same span length. This will be further explained in the subchapter geometry.

The load effect is the same for all three bridge types. The main focus is on variable loads and permanent loads such as: self-weight, traffic load and earth pressure, as these actions make up the majority of the load effects. The calculations refers to load effects and preliminary sizing of a simply supported superstructure (as design loads and design resistance).

One exception is made in terms of load effect from traffic load for the steel-concrete composite bridge, where the dominant sectional forces have been extracted using the software program Strip Step 2 (Bengtsson & Wolf, 1969), enabling the optimization of multiple cross-sections on the same bridge. This can be further described in Section 3.5.1.

Each bridge is constructed using parametric design with MathCAD Prime 8 and MathCAD Prime 9 as programming tools (PTC, 2023). Each bridge has its own optimization preferences to minimize material usage considering LCA, which are described under each bridge's respective subheading as follows.

Input to these MathCAD tools, in addition to the optimization preferences, is the geometry in the form of the carriageway width and span length of the bridge. Mass of materials and CO_2-equivalents for steel and concrete are collected for bridge widths of 6, 9 and 12 meter for every other meter length from a span length of 6 to 40 meter. Further explanations are given under subheadings for each bridge. The optimization tools resulting from the study are available for review by Svensson and Pålsson (2023).

3.1 Loads acting on superstructure

Load effecting the superstructure originates from self-weight of the superstructure, self-weight of the from wing wall and end shields, traffic loads, and earth pressure. The load effects are calculated as worst case scenarios for moment and shear force. Preliminary sizes of the superstructure for all three bridghes are designed according to these. The load effects are calculated per meter (b) bridge and so is the resistance of the cross-section.

Below is some deceptive pictures of the simplified structural model and the loads effecting the cross-section for moment in the ULS, which applies for all bridge types. The figure below describes a superstructure with a span under 22.4 meter, where LM1 is governing as variable load for moment (Figure 3.1 and 3.2).

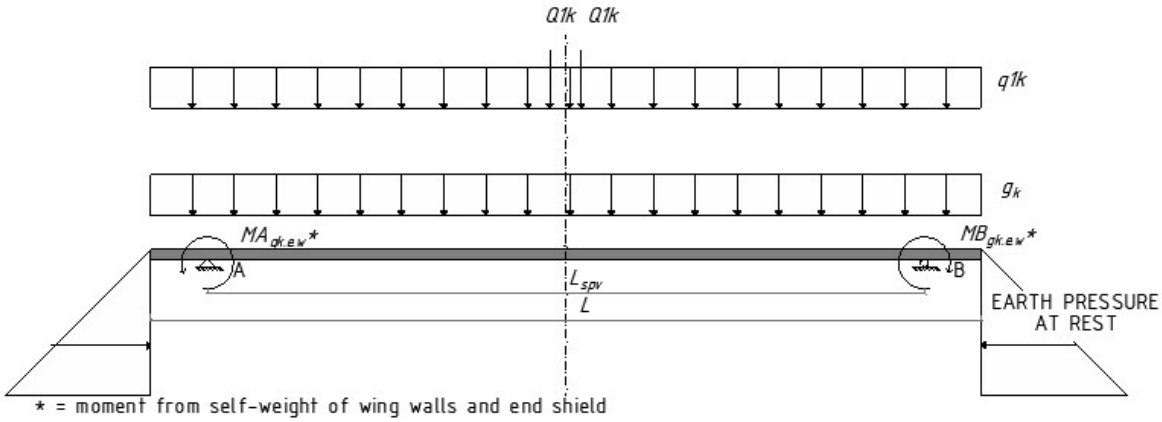

Figure 3.1: *Structural model and load effects.*

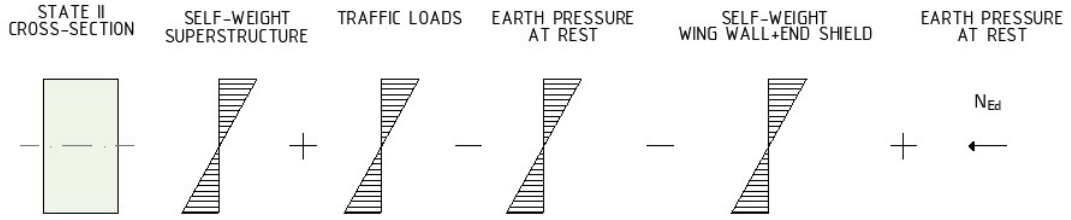

Figure 3.2: *Moment and normal force acting on the cross-section in State II.*

3.1.1 Variable load (Q)

LM1, LM2 and vehicle models A-O were iterated in the span of 6-40 meter with 0.1 meter steps to determine the worst load case for each length. In this step when comparing the load cases against each other the carriageway is set to 3 meter and for the vehicle model the dynamic factor is set to 25 %. For all load models, the load was tested in both forward and backward directions.

3.1.1.1 Traffic load

Moment:
To conclude when to use which specific load case for worst case moment, each load case for span lengths are collected and presented in Figure 3.3.

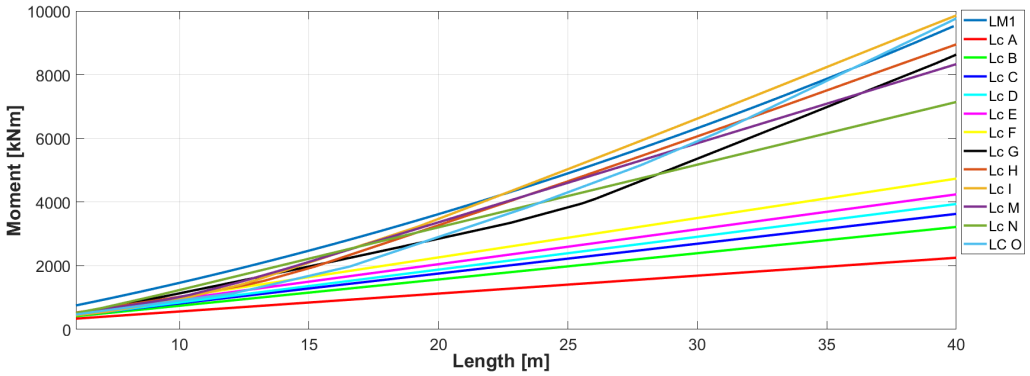

Figure 3.3: *All load cases.*

The load case that is dominant for each span length is presented in Figure 3.4, and shows that the most unfavourable cases for each span is:

- 6.0 m $< L_{spv} \leq$ 22.4 m $\rightarrow$ LM1
- 22.4 m $< L_{spv} \leq$ 40 m $\rightarrow$ Vehicle model I

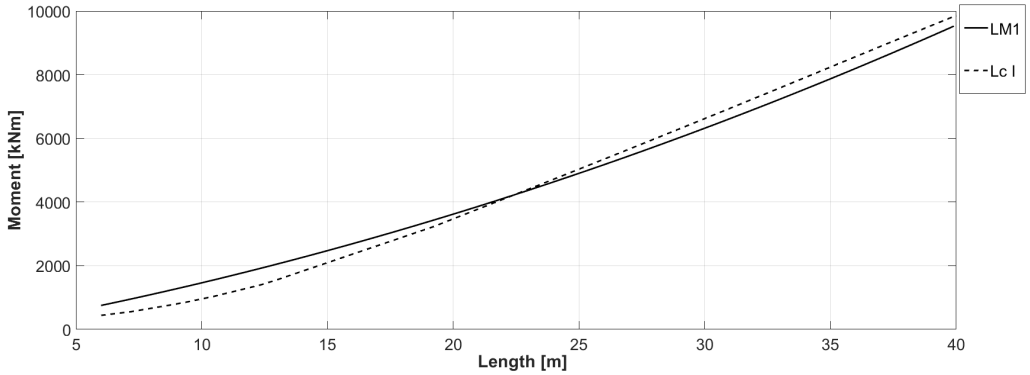

Figure 3.4: *Load case with highest moment.*

The worst case scenario for moment corresponds to the placement of LM1 and Vehicle load I to the figures below (Figure 3.5 and Figure 3.6).

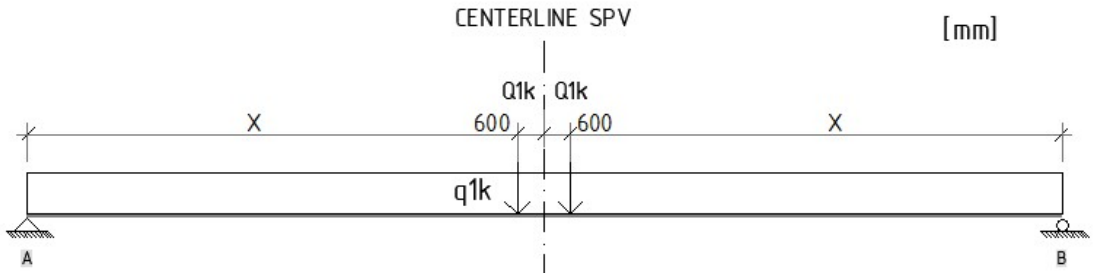

Figure 3.5: *Position of Load model 1.*

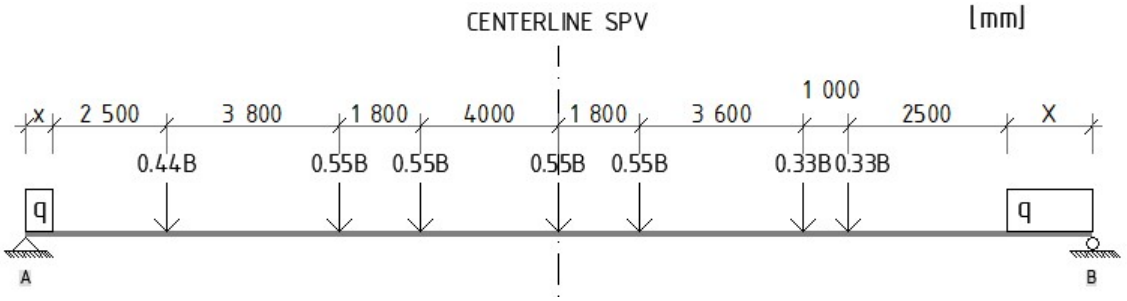

Figure 3.6: *Position of Vehicle load I.*

Shear:
To conclude when to use a specific load case for worst-case shear force, each load case for span lengths is collected and presented in Figure 3.7. The worst shear force in a beam develops at one of the supports. But in reality shear forces do not develop closer then 0.9 d (90 % of the effective height) to the support. This is because shear forces will be transferred with arch action directly to the support, and not as shear force in the beam. In this study, the shear force is calculated directly at support, which is not realistic, but considered conservative since it is larger in magnitude.

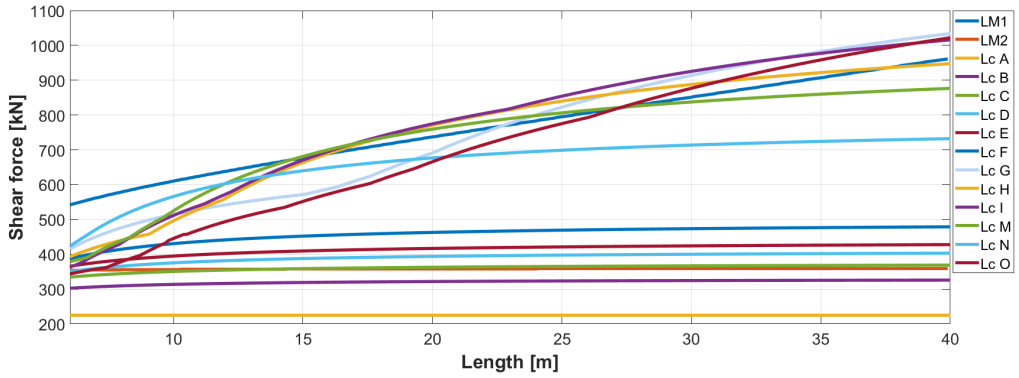

Figure 3.7: *Shear force with different span lengths and load cases.*

The load case that is dominant for each span length is presented in Figure 3.8. The study shows that the most unfavorable case for length beam applies:

- 6.0 m $< L_{spv} \leq$ 14.5 m $\rightarrow$ LM1
- 14.5 m $< L_{spv} \leq$ 16.9 m $\rightarrow$ Vehicle model M
- 16.9 m $< L_{spv} \leq$ 33.3 m $\rightarrow$ Vehicle model I
- 33.3 m $< L_{spv} \leq$ 40.0 m $\rightarrow$ Vehicle model G

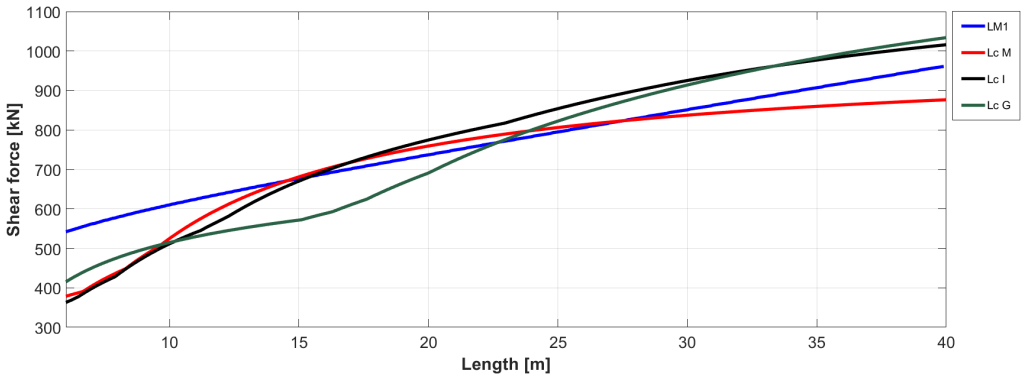

Figure 3.8: *Max shear force at different span length.*

The worst-case scenario for shear corresponds to the placement of LM1, Vehicle load M, Vehicle load I, and Vehicle load G in the figures below.

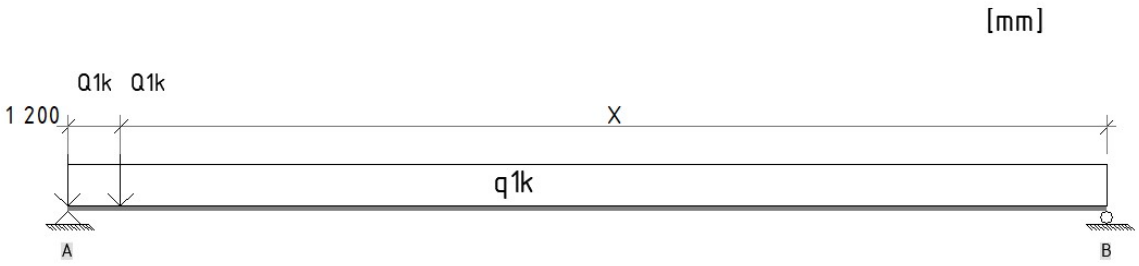

Figure 3.9: *Position of Load model 1.*

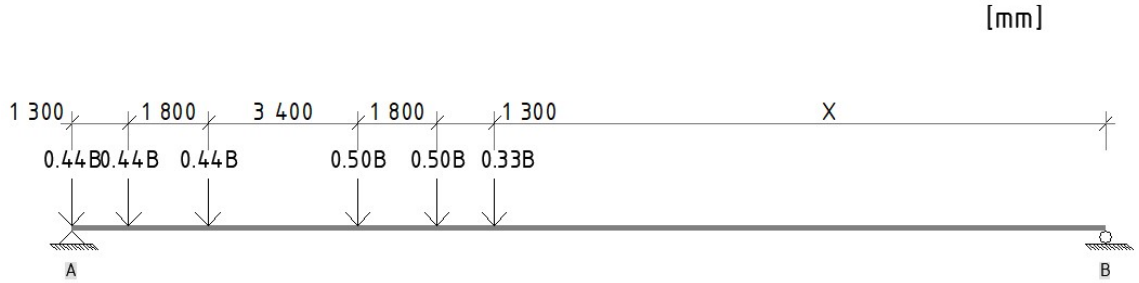

Figure 3.10: *Position of Vehicle load M.*

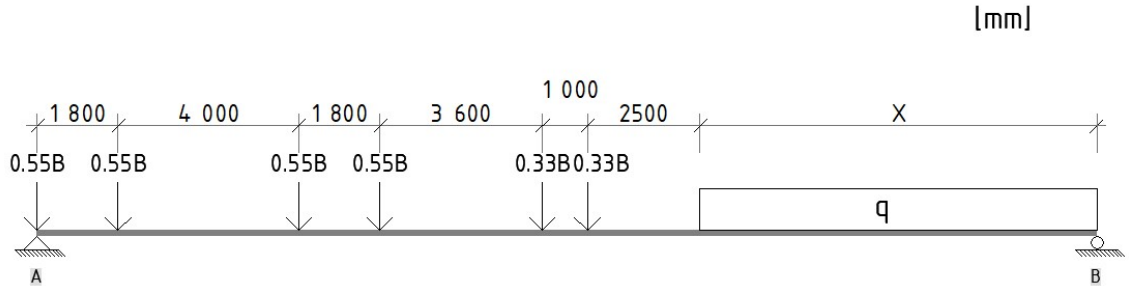

Figure 3.11: *Position of Vehicle load I.*

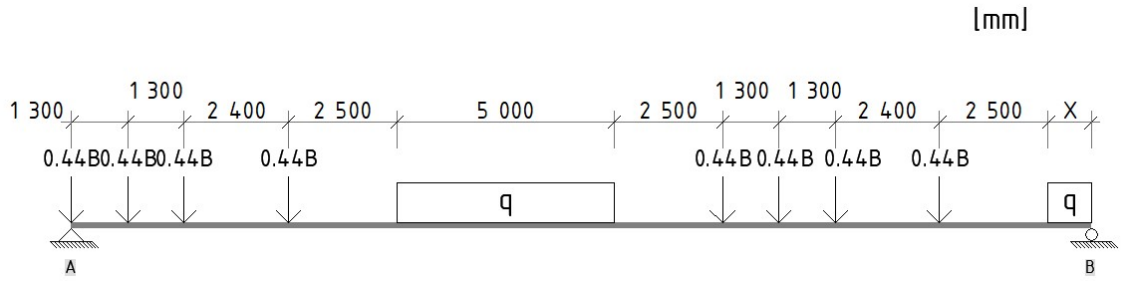

Figure 3.12: *Position of Vehicle load G.*

3.1.2 Permanent loads (G)

3.1.2.1 Self-weight

Self-weight acts on the bridge in the form of, self-weight superstructure, self-weight pavement, self-weight wing walls, and self-weight end shield. These provide a load effect in the form of moment and shear force. The self-weight of the superstructure and pavement acts as a distributed load (q) over the entire superstructure and produces an unfavorable moment within the span L_{SPV} and a favorable moment outside of the supports (see Figure 3.13). These loads results in shear forces in the beam (which in this case are calculated at support A).

The dead weight of the wing walls and the end wing act on either side of the supports, with a cantilever to the end wing, both as favorable moments. These do not contribute to the maximum shear force that sizes for.

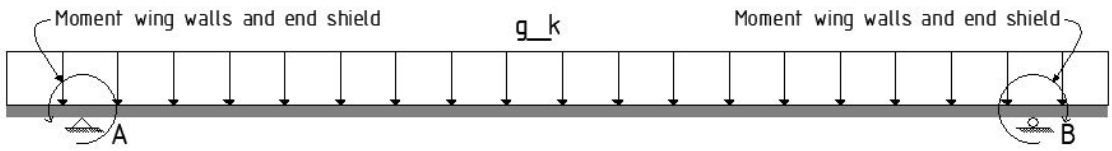

Figure 3.13: *Position of Vehicle load G.*

3.1.2.2 Earth pressure

Earth pressure at rest acts as a permanent load against the end shield (this is further explained in chapter 3.2). Earth pressure at rest increases proportionally to depth and is highest at the bottom of the end shield. The load provides a favorable moment and normal force (see Figure 3.14).

Figure 3.14: *Earth pressure at rest acting on the end shields.*

3.2 Geometry

The geometry of the end shield is determined by the combined horizontal displacement from the temperature change (highest to lowest in a year), braking, and overload. The height of the end shield must be at least 200 times the displacement of the respective end shield (see figure below). The contribution from braking and overload is assumed to be +20 % of the contribution from the temperature change (which is considered a conservative value).

The height of the end shield must be at least 1.5 meter.

This geometry of the wing walls is then a function of the geometry of the end shield, the inclination 1:1.7, and the fixed dimensions presented in the section below.

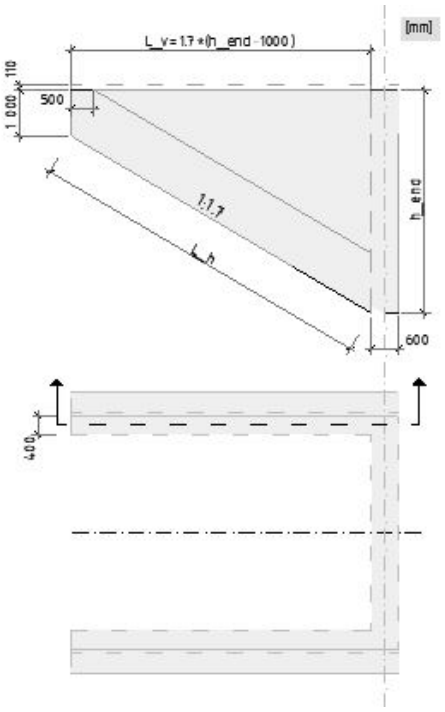

Figure 3.15: *Section of end shields and wing walls.*

3.2.1 Reinforcement design for construction elements common for all bridge types

The design of the following construction elements is not affected by the change of span length or width, therefore it's only necessary with one reinforcement design for the three bridge types. The reinforcement amount and layout have been developed with Inhouse Tech Göteborg AB and where drawings of existing bridges have been used as a basis.

3.2.1.1 Wing wall

The wing wall needs reinforcement in both vertical and horizontal directions to transfer the horizontal load from the backfill soil and the vertical load from self-weight and traffic load.

Longitudinal reinforcement is designed with two different bar sizes and center-to-center measurements and is presented in Figure 3.16 and 3.17.

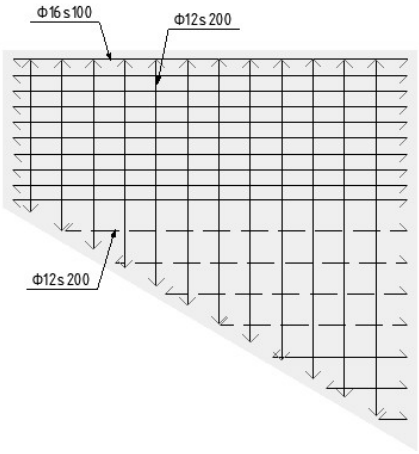

Figure 3.16: *Elevation of reinforcement design wingwall.*

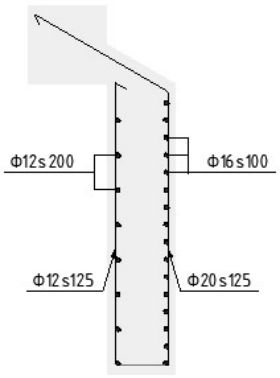

Figure 3.17: *Section of reinforcement design wingwall.*

3.2.1.2 End shield

The end shield is subjected to horizontal forces from the traffic load and the backfill soil, to transfer the favorable moment and normal force to the superstructure and to fulfill the requirements regarding deformation and resistance a reinforcement design has been developed.

The end shield is mainly subjected to permanent loads and the magnitude isn't affected by the span and width of the superstructure, the result is presented in Figure 3.18.

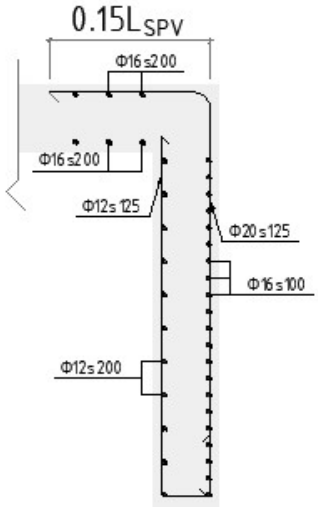

Figure 3.18: *Reinforcement design end shield.*

3.2.1.3 Edge beam

The design of reinforcement in the edge beams is equal for all span lengths and widths, edge beams are designed to resist accidental loads.

Longitudinal reinforcement in the edge beam is determined to be 10 bars with a diameter of 16 mm. The shear reinforcement is designed as vertical stirrups with a diameter of 10 mm and the placement in the longitudinal direction is every 200 mm.

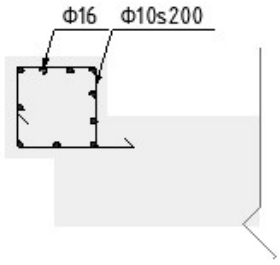

Figure 3.19: *Reinforcement design edge beam.*

3.3 Slab bridge

The main goal of designing the slab bridge is to achieve an optimized cross-section regarding CO_2-equivalents. Studies made in Alhede and Beskow (2020) proves that slenderness is the governing parameter to reduce the carbon impact, a bridge with higher slenderness will have less concrete and more reinforcement and is sufficient as long it is constructability and the lever arm from the tensile reinforcement is effective.

3.3.1 Way of bearing

The superstructure consists of a slab and since it's simply supported on two edges it can be defined as a one-way slab that mainly carries the load in one direction and is statically determined (Engström, 2014). The slab is divided into strips with a unit width and each strip can be designed with Euler-Bernoulli beam theory.

3.3.2 Reinforcement design superstructure

As mentioned before a high amount of reinforcement gives a lower CO_2-equivalents footprint than a cross-section with a lower amount of reinforcement and higher construction height. With that as a basis, a cross-section with the maximum possible amount of reinforcement has been selected with regard to constructability, either in one or up to four layers of reinforcement. All reinforcement is designed with the lap splice length as $50 \cdot \phi$.

At lower span widths, it is convenient to use one layer of reinforcement to take advantage of the longer lever arm from the tensile reinforcement and is presented in Figure 3.20). At longer spans, one layer of tensile reinforcement will not be enough, and therefore one or more additional layers are added that are placed parallel to the first layer see Figure 3.21 - 3.23). The reinforcement dimension is chosen to ϕ 25 mm with the lowest possible distribution s125 mm in regards to constructability. The concrete cover to the first layer of tension reinforcement is calculated taking into account anchoring, durability, stirrups, and reinforcement size.

The shear reinforcement is designed as vertical stirrups with the dimension ϕ 16 mm, and the center-to-center distance between the stirrups is set to 625 mm. The placement of stirrups in the longitudinal direction is decided in the calculation part to get as high utilization rate as possible for the shear reinforcement.

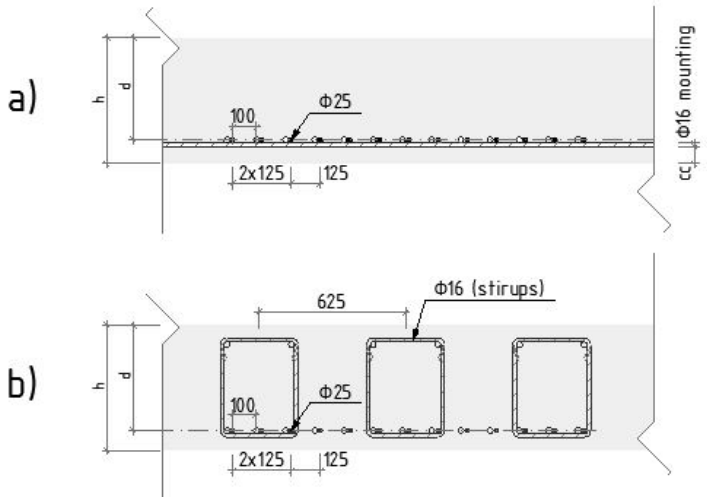

Figure 3.20: *Reinforcement design with 1 layer of tension reinforcement. a) section without shear reinforcement. b)section with shear reinforcement.*

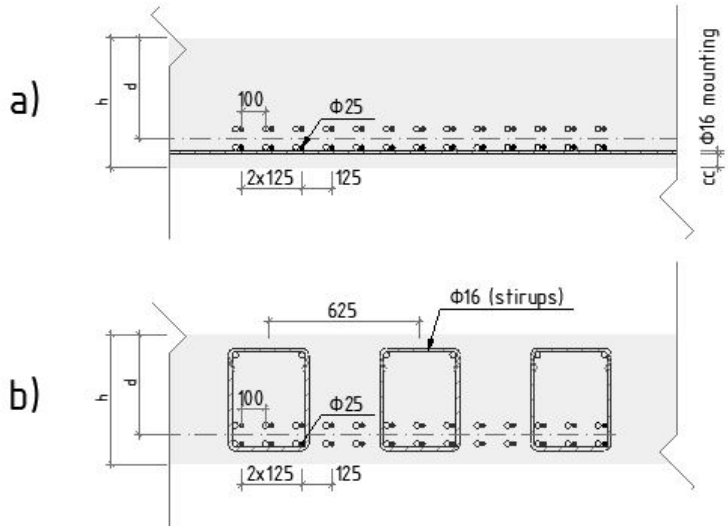

Figure 3.21: *Reinforcement design with 2 layers of tension reinforcement. a) section without shear reinforcement. b)section with shear reinforcement.*

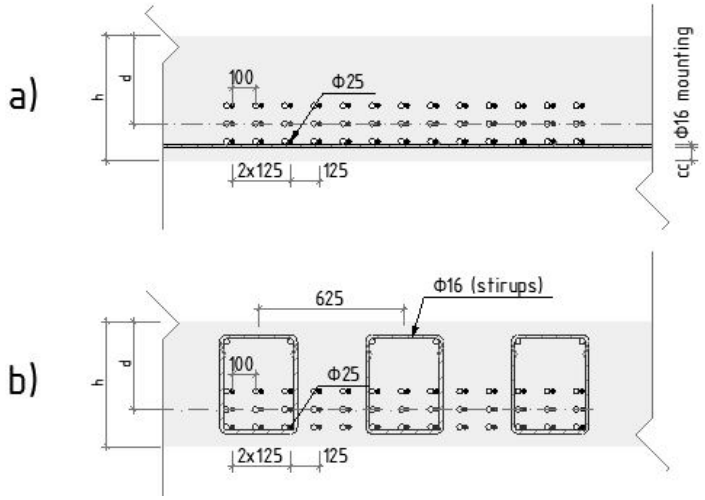

Figure 3.22: *Reinforcement design with 3 layer of tension reinforcement. a) section without shear reinforcement. b)section with shear reinforcement.*

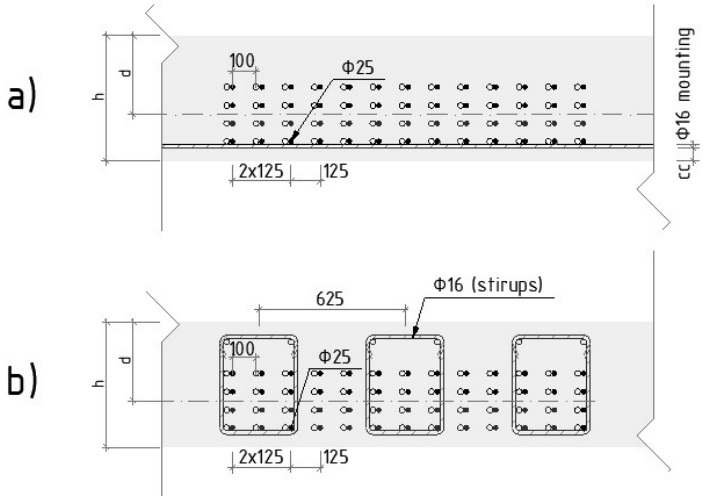

Figure 3.23: *Reinforcement design with 4 layer of tension reinforcement. a) section without shear reinforcement. b)section with shear reinforcement.*

3.3.3 Reinforcement curtailment

The reinforcement curtailment is designed both for tension- and shear reinforcement, the main goal is to reduce the amount of reinforcement in sections where the shear and moment capacity is sufficient with a lower amount of reinforcement.

To simplify the calculations a distributed load is calculated from the critical moment in the field, with the new distributed load it can be determined where in span a reduction with one layer of reinforcement can be made.

In the sections where the concrete can take all the shear force and still fulfill the demands for shear capacity the shear reinforcement amount is reduced to the calculated minimum amount according to (CEN., 2005a).

3.3.4 Deformation checks in SLS

Deformation checks in SLS are made in frequent load combination and the slab is considered cracked. To simplify the calculations, flexural rigidity is calculated as the cross-section is uncracked and reduced by 40 %. Comparison was made with "FEM calculations in Brigade plus" and the conclusion was made that the contribution of stiffness is greater than expected for rotation at support, therefore the calculation was made with the mean load from 2 traffic lanes.

According to Trafikverket (2022) should the vertical deformation be controlled with only variable loads, and there are two controls that need to be checked. The maximum deflection in the span is calculated with the elementary case for simply supported beam and the deflection should be less or equal to $L_{spv}/400$ to achieve a comfortable and safe feeling for the passengers. The maximum deflection in the cantilever is determined by calculating the support rotations and the maximum

deflection in the cantilever should be less or equal to 5 mm.

3.3.5 Resistances checks in ULS

Calculation of the stress limitation is made in state II, assuming a cracked section with a linear elastic material response until the maximum capacity has been reached. The bending moment capacity is governed by the height of the slab and the amount of tension reinforcement, a larger height of the slab gives a larger lever arm for the tension reinforcement. The calculations are made in the worst section in the longitudinal direction of the slab and therefore only the max amount of needed tensile reinforcement and slab height is determined. When optimizing the superstructure in further chapters to conclude the GWP, tension reinforcement will be optimized for specific sections in more detail to fulfill the bending moment.

The shear resistance is determined in section $0.9 \cdot d$ from each support, for short bridge spans it may be enough with shear resistance from the concrete slab. If the concrete slab doesn't have enough shear capacity shear reinforcement is used and they are designed as stirrups. The center-to-center distance between the stirrups is constrained to 625 mm regarding constructability. The distance between the stirrups in the longitudinal direction is a free variable to utilize the shear capacity. At a certain distance from the support shear reinforcement won't be necessary due to the concrete slab can take all of the shear force but this will be presented in further chapters.

3.3.6 Input data MathCAD tool

The calculation for the checks mentioned in this chapter is made in a MathCAD script, where the input is the span length, the width of the bridge, the height of the concrete slab, and the thickness of the pavement. The output consists of utilization rates for the different checks and the amount of CO_2-eq for both the superstructure and for the bridge including the end supports. As mentioned in previous chapters, the span length between 6-40 meter and bridge width of 6-12 meter will be investigated. To find out the most optimal cross section for each span length and bridge width an iteration in the MathCAD script is executed and the workflow is described in Figure 3.24.

To simplify the iteration process each change of the height of the slab height is limited to 10 mm. If the deformation checks are not satisfied, the height of the concrete slab is increased. In case of insufficient moment capacity, the amount of tension reinforcement is primarily increased, and if the maximum layer of tension reinforcement is reached, the height of the concrete slab is increased.

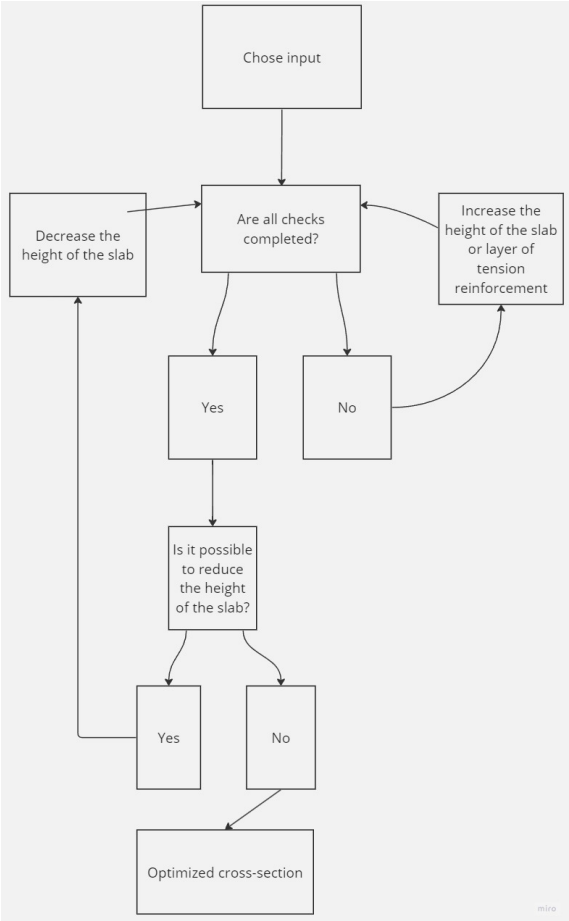

Figure 3.24: *Iteration method for slab bridge.*

3.4 Girder bridge

The cantilevers is designed with a maximum length of 2.5 meters from the edge beam to the primary beam. This is strategically chosen as a max length to minimize the load effect of to half the vehicle's axles (as in figure 3.22). This is considered in the industry standard to get a reasonable cross-section for the cantilever in the ultimate limit state.

The maximum height of the main girder is considered to be $L_{spv}/20$ and the minimum height $L_{spv}/30$. This is because prestressed bridges are the main option when the construction height needs to be limited.

An optimized cross-section for the girder bridge referring to LCA (see Figure 3.25), should be the minimum possible width of the primary girder, combined with the maximum length of cantilever arms (covering the total width of the carriageway.) (still fulfilling $B \leq 5H$).

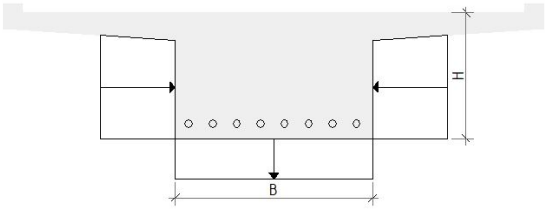

Figure 3.25: *Optimised cross-section referring to LCA.*

When the effective height still does not have the capacity to carry the load effect, the width can be increased to allow spacing for more tendons. But this is a secondary choice, since this will lead to more material use, as in the figure above.

3.4.1 Way of bearing

The superstructure consists of a girder with prestressed reinforcement with cantilevers on each side. The girder carries the load in the longitudinal direction with beam action to the supports at each end, and the cantilevers transfer the load to the girder in the transverse direction. The placement of the prestressed reinforcement follows the moment curve for the girder, close to the support where there is a negative moment placed at the top of the girder.

3.4.2 Reinforcement design superstructure

The prestressing tendons are placed inside ducts, and the ducts are positioned with a curve to constitute maximum auxiliary moment in field (maximum eccentricity to the center of gravity), where moment is at the largest magnitude, as shown in Figure 3.26. It is also placed with such an inclination to be able to provide a force vector that helps support a part of the shear force. The first and last meter is inserted completely horizontally for practical reasons.

Section B (Figure 3.26) shows the distances between ducts for the cross-section. The number of ducts is chosen to cope with the moment in the SLS for the selected cross-section (without any tensile stresses), alternatively the maximum number of ducts according to the distances specified below. Each duct has a diameter of ϕ105 mm and contains multi-strand tendons with 19 strands of size ϕ15.7 mm.

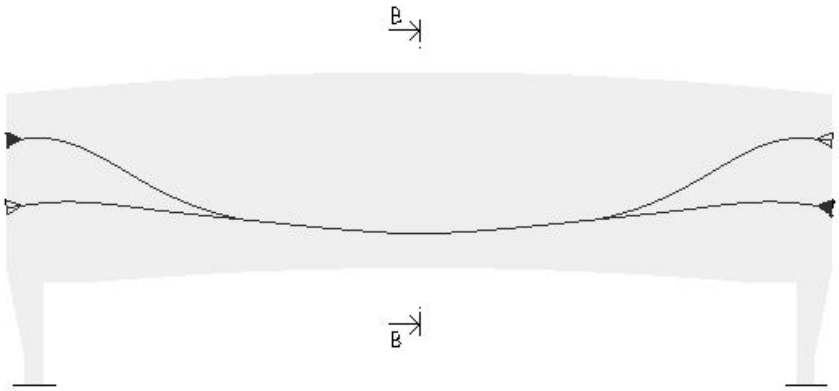

Figure 3.26: *Prestressing tendon profiles.*

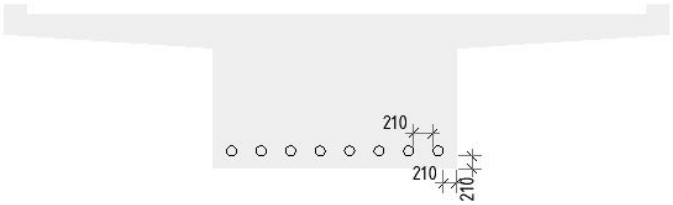

Figure 3.27: *Section B.*

Shear reinforcement is designed as stirrups and to evaluate the shear resistance in the girder a mean value for the distance between the stirrups is set to 425 mm, the distance between the stirrups in the longitudinal direction is a free variable to utilize the shear capacity.

To resist the torsional moment, longitudinal reinforcement is designed with a diameter of ϕ20 mm and is placed evenly distributed in the cross-section along the edges see Figure 3.28.

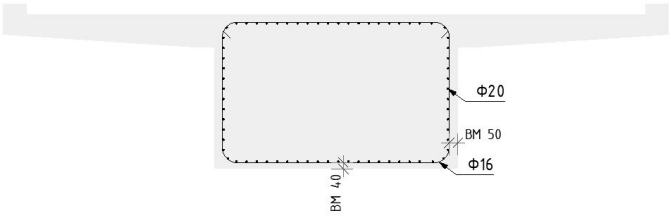

Figure 3.28: *Placement of torsional moment reinforcement.*

The tensile reinforcement in to resist the moment in the cantilever is fixed to ϕ16 mm with a spacing of 100 mm. The free variable to get the highest utilization rate in this case is the effective height.

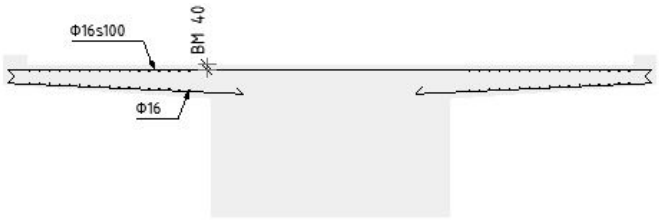

Figure 3.29: *Cantilever reinforcement.*

Shear and dowel reinforcement is a unique type of reinforcement specifically designed for pre-stressed concrete beam bridges and should therefore be included in the LCA. The input data for this reinforcement is partially based on experience and partially parameter-driven. The cross-sectional dimensions of the reinforcement are based on experience while the length and number of pre-stressed cables can be parameter driven, this varies and is further described in Figures 3.30 and 3.31.

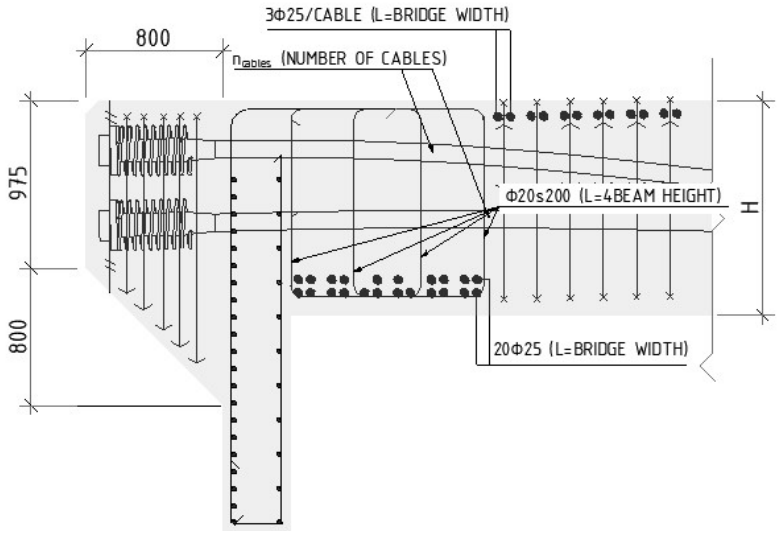

Figure 3.30: *Section of shear and dowel reinforcement.*

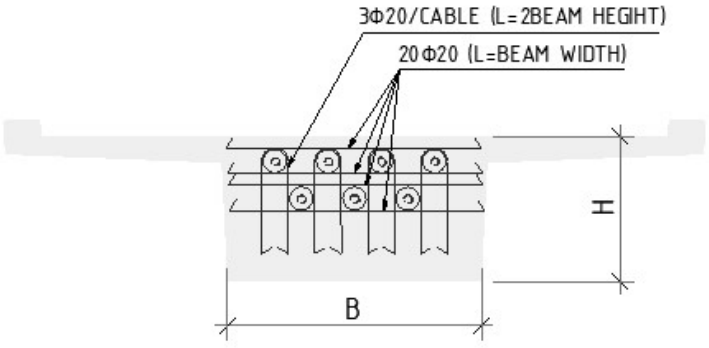

Figure 3.31: *Section of shear and dowel reinforcement, beam.*

3.4.3 Stress limitations in SLS

The girder will be designed to resist certain stress limitations in both frequent- and quasi-permanent load combination. In terms of mitigating the potential for excessive creep deformations in concrete, it is essential to impose restrictions on the compressive stress of the concrete during both the application of prestressing to the structural element and the presence of the quasi-permanent load (Engström, 2011). Under quasi-permanent load combination, there is a risk of cracking and too high compression, at the top of the cross-section. For the sake of simplicity, dimensions are calculated as in state I.

The quasi-permanent load combination is also used for short-term response, where compression at the bottom and tension at the top are critical. In this load combination, only prestressing and permanent loads are considered, and cross-sectional properties are taken without creep, shrinkage, and relaxation.

In frequent load combination there is a risk of cracking at the bottom of the cross-section due to tensile stresses. Usually no cracks are allowed 100 mm from the ducts. But in this study the cross-section is calculated in state I, where no tensile stresses are allowed at the outer part of the girder, as a conservative and simplified approach.

Maximum tensile stress under frequent load combination is allowed to amount to f_{ctm} in case of one inoperative tendon cable.

3.4.4 Resistances checks in ULS

3.4.4.1 Cantilever

The cantilever is designed for the shear force and moment that occurs in the ULS where the cantilever length is a maximum of 2.5 meter (from primary beam to edge beam). The worst load effect originates from the fictitious vehicles LM1 and LM2 for load lane 1 see Figure 3.32.

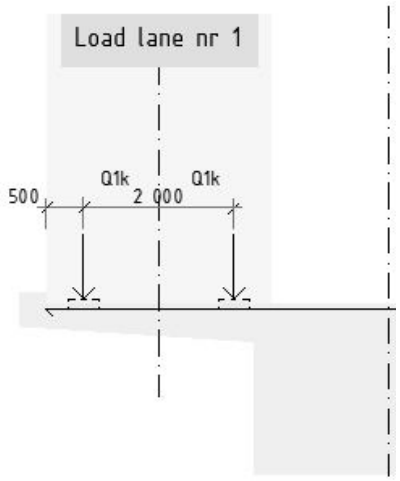

Figure 3.32: *Cantilever load lane 1.*

When the vehicle is positioned centrally in the load lane 1, one wheel load is placed 500 mm from the edge beam. The critical cross-sections for moment is just at where the cantilever connects to the primary beam. For the shear force, there are two critical cross-sections, firstly cantilever meets the primary beam and secondly at the position of the point load. This is because the shear capacity and shear force increases closer to the main beam due to the changing height of the cross-section (increased height cross-section and increased self-weight).

The moments arising from an vehicle axis are calculated with the load distribution (r) against the fixed section, which is the length in depth, transverse to the tensile reinforcement (Figure 3.33). Where r is calculated according to *Bestämmelser för betongkonstruktioner: Allmänna konstruktionsbestämmelser* (Statens betongkommité, 1969).

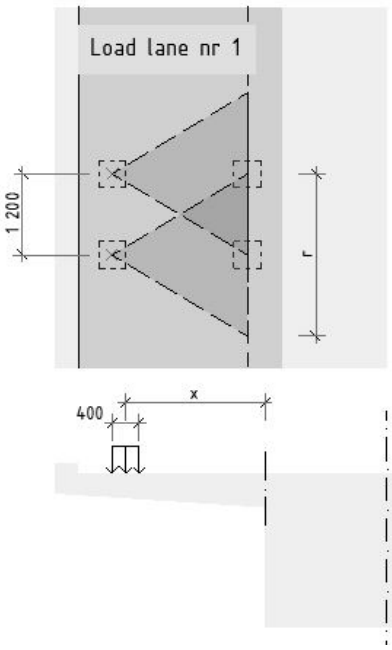

Figure 3.33: *Distribution of moments for load model 1.*

Correspondingly, the distribution for shear force is calculated as *Recommendations for finite element analysis for the design of reinforced concrete slabs* (Pacoste, Plos, & Johansson, 2012) which is based on finite element empirical studies for cantilever bridges. The distribution of shear force in the critical section is calculated as the effusive width Figure 3.34.

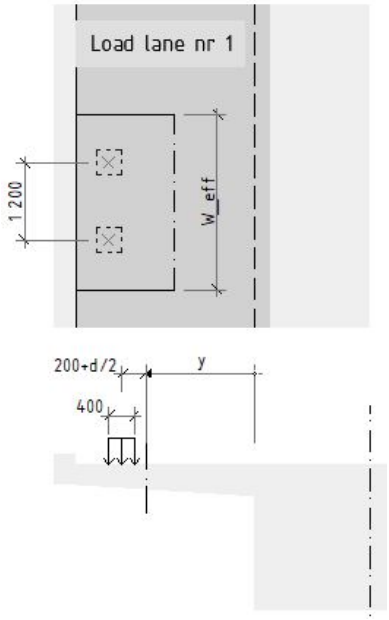

Figure 3.34: *Distribution of shear force for LM1.*

With reference to build-ability and standard, the edge beam is determined as to 450x450 mm, as described earlier. Where the edge beam connects to the cantilever, a fixed height of the cross-section is determined to be 235 mm also, with reference to build-ability. The free variable in the cross-section (that can be varied in order to gain capacity) is where the cantilever connects to the primary beam.

3.4.4.2 Girder

The girder should fulfill the demands on resistance against shear force and torsional moment and the combination of them both see Equation 3.1. The maximum design shear force is calculated with the associated torsional moment for the load case and the same procedure is repeated for the design torsional moment as in Figure 3.35 with reference to 6.3.2 in (CEN., 2005b).

$$\frac{T_{Ed}}{T_{Rd,max}} + \frac{V_{Ed}}{V_{Rd,max}} \leq 1 \tag{3.1}$$

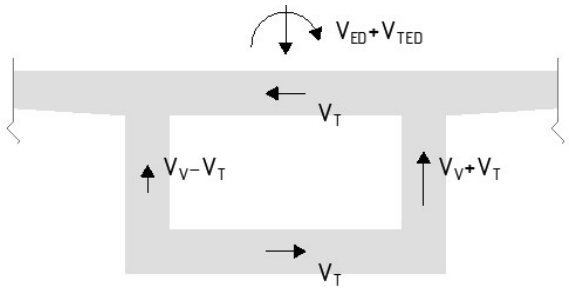

Figure 3.35: *Example of the combined effect of torsional moment and shear force.*

Torsional moment occurs due to non-symmetrical traffic loads along the width of the bridge, for LM1 both the point loads and distributed load will have a different magnitude between the traffic lanes see Figure 3.36. Vehicle load models are designed as the point loads have the same magnitude in two of the traffic lanes and the distributed load is equal along the width of the bridge see Figure 3.37.

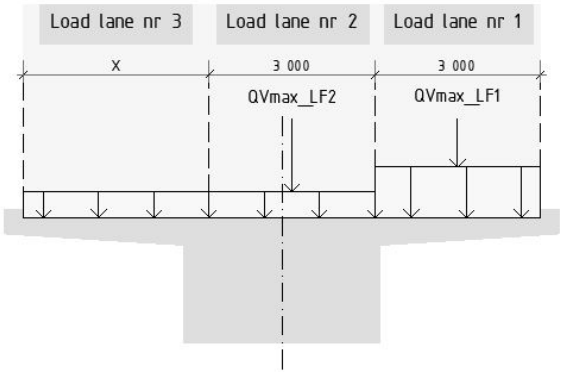

Figure 3.36: *Load model 1.*

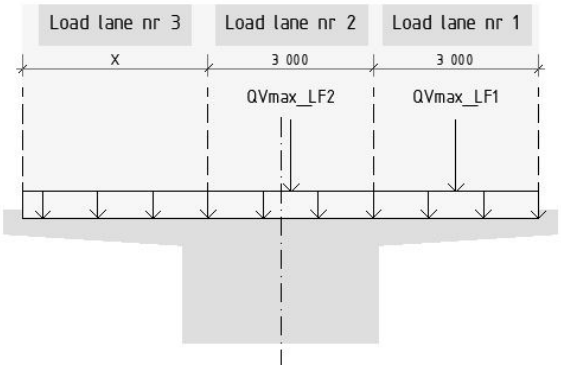

Figure 3.37: *Vehicle loads.*

The shear resistance is checked for the girder in ULS according to (CEN., 2005a). To evaluate the worst-case scenario it is assumed that the girder is cracked. For pre-stressed concrete members with an inclined tendon, a favorable shear force can be included and reduce the design shear force, due to the vertical force vector (Engström,

2011).

The favorable shear force is calculated by a simplified approach, collecting data from recent project at Inhouse Tech Göteborg AB. A minimum favorable effect was derived as 7 % of the prestressing force. The shear capacity in a cracked concrete section without shear reinforcement is determined by calculating the shear sliding failure, if the section has sufficient resistance should the minimum reinforcement amount be used according to (CEN., 2005a).

The design of shear reinforcement is checked against shear sliding failure with yielding shear reinforcement, the design of the shear reinforcement is done by a truss model with variable strut inclination (Engström, 2011). The inclination considered in this study is set to the minimum value 21.8 degrees.

3.4.5 Input data MathCAD tool

As described earlier in the report, widths of 3, 6, and 12 meters are optimized every other meter from 6 to 40 meters. A limitation is that the cables must fit within the height restriction of the beam (h_{max}), which is a percentage of the length ($L_{spv}/20$). Therefore, the girder bridge is optimized for every other length meter L_{spv} from 14 to 40 meters. At 14 meters, the minimum possible height (h_{max}) is achieved to accommodate the tendons.

The program will recommend a number of tendons that can be used to withstand the frequent traffic loads. However, this value is based on equilibrium in the height of the tendon cables (up-rounded), and will maybe not result in zero tension or compression in bottom of the cross-section.

For each L_{spv}, the optimized cross-section is determined with the maximum possible cantilever length, the minimum possible height h_{min}, and the minimum possible width is b_{min}. However, these minimum cross-section does not hold for one or several ULS and SLS checks, therefore the cross-section needs too be iterated in a specific order, which are mentioned below.

Initially, **(1)** the height is increased from h_{min} towards h_{max} by 0.01 meters at a time (with the recommended number of tendons to withstand frequent traffic loads). If the bridge does not withstand the frequent traffic load (no tension allowed in bottom mid span), the number of cables is increased by **(2)** adding +1 tendon for each step until zero tension or compression in the bottom is reached. If this can not be met with the specific width, **(3)** the cantilevers are reduced (and the width increased correspondingly) by 0.1 meters at a time until the number of tendons needed fits (maximum number of tendon cables that fits is displayed and is updated as the width increases). Maximum beam width allowed is ($B \leq 5H$).

If the quasi-permanent load combination for short-term response (compression at the bottom, mid span) is a limitation for the specific span length, **(3)** the cantilevers are reduced by 0.1 meters at a time, increasing the moment of inertia (stiffness) of the beam and its self-weight, which reduces the compression at the bottom in the quasi-permanent load combination.

If the deflection of the cantilever is the limiting factor (SLS - traffic loads), **(3)** the width of the beam is iteratively increased by 0.1 meters at a time until to the moment of inertia (stiffness) of the beam reduces the deflection to 5 mm or less (provided that the maximum height of the beam is already implemented).

A simplification of the iteration-process is described in Figure 3.38. Initial cross-section layout can be seen Table 3.1.

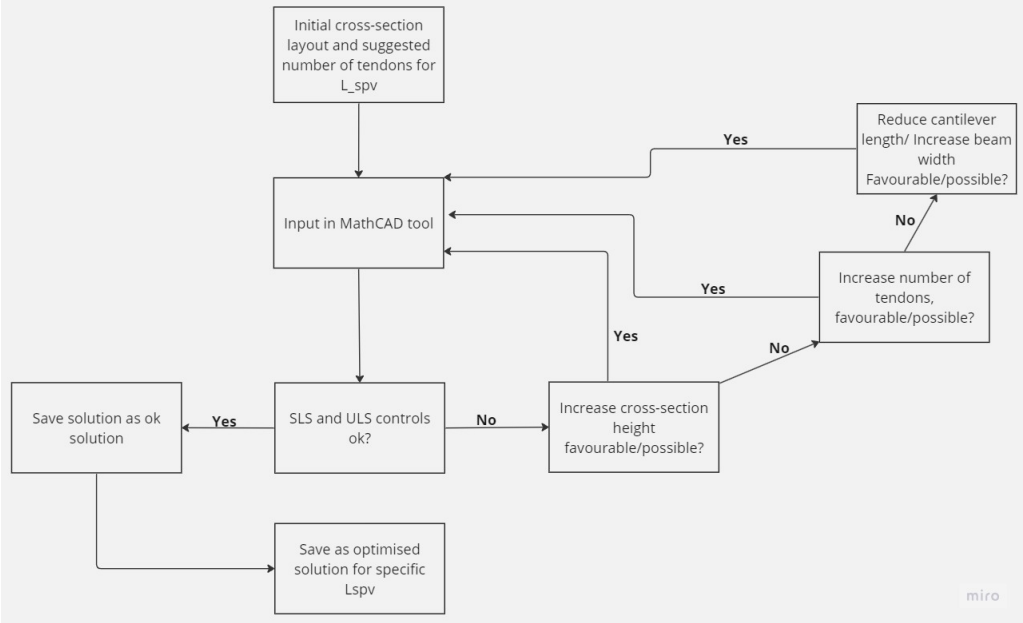

Figure 3.38: *Simplification of iteration-process of girder bridges.*

Table 3.1: Start input-data for MathCAD tool for girder bridge

L_{spv} [m]	h_{max} [m]	h_{min} [m]	b_{max} [m]	b_{min} [m]	$L_{cant.max}$ [m]
14	0.7	0.47	3.5	3.5	2.5
16	0.8	0.53	4.0	3.5	2.5
18	0.9	0.60	4.5	3.5	2.5
20	1.0	0.67	5.0	3.5	2.5
22	1.1	0.73	5.5	3.5	2.5
24	1.2	0.80	6.0	3.5	2.5
26	1.3	0.87	6.5	3.5	2.5
28	1.4	0.93	7.0	3.5	2.5
30	1.5	1.00	7.5	3.5	2.5
32	1.6	1.07	8.0	3.5	2.5
34	1.7	1.13	8.5	3.5	2.5
36	1.8	1.20	9.0	3.5	2.5
38	1.9	1.27	9.5	3.5	2.5
40	2.0	1.33	10	3.5	2.5

3.5 Steel-concrete composite bridge

As a basis of design of the steel-concrete composite bridge, some initial assumptions are made about the bridge configuration, including the length of the cantilevers. Industry standards, as specified in BATMAN (Trafikverket, 2008), recommend that the length of the cantilevers be 0.4 times the distance between the main beams (as in 3.39.

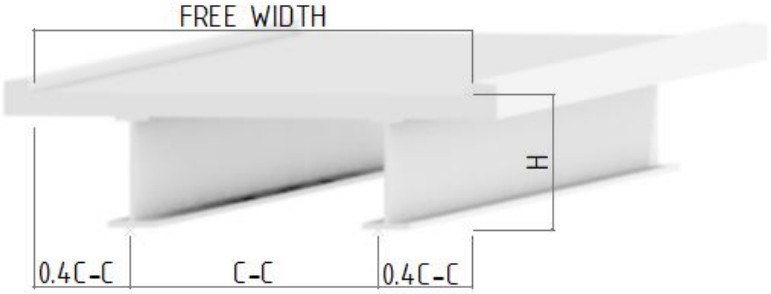

Figure 3.39: *Section composite bridge element(s).*

The cantilevers are crucial components in the design process. They are typically designed with a maximum length of 2.5 meters, measured from the edge beam to the primary beam. This length has been strategically chosen to minimize the load effect of up to half of the vehicle's axles. The industry standard considers this design consideration as a means to achieve a reasonable cross-section for the cantilever in the ultimate limit state. Additionally, the cantilevers are designed to carry both the dead load of the bridge's own weight and the variable load of vehicles passing over it. Therefore, the design of the cantilevers is critical to ensure the bridge's structural integrity and safe operation. The design process of the cantilevers is further

described in Section 3.4.4.1.

In the designed steel-concrete composite bridge, the concrete cross-section between the main beams is this case designed with the same cross-section height as the cantilevers, which concludes a constant cross-section of the concrete deck. However, it is important to note that this design approach is a simplification, as the actual cross-sections may differ due to varying loads and other design considerations that are not included in this study.

However, in future studies, it would be interesting to explore the potential benefits of adjusting the cross-section height of the concrete between the main beams to reduce the total amount of cubic concrete used in the bridge.

Steel beams are used as the main load-carrying members of the bridge superstructure with or without composite action with the concrete slab. To optimize the performance of the steel beams, they are divided into three sections, support section at the ends and a field section in the middle. These sections are designed to be optimized for the associated load effects for moments and shear forces, with a limitation of constant total height of the beams, for practical reasons and how this is calculated is further described in Figure 3.43. these three beams are welded together see Figure 3.42. The first support section starts from 0 meters and to determine the length of the beam, an equation has been developed based on previous projects, where a minimum dimension of the outermost beam (L_{el}) is obtained see Equation 3.2.

$$L_{el} = \frac{L_{bridge} - 18m}{2} - 1.3m \tag{3.2}$$

Besides welding the three beams together, vertical stiffeners are welded at supports and to decide a reasonable c-c distance studies on similar previous bridges has be done, the conclusion was that a c-c distance of 6.5 meter was reasonable but to get a symmetrical cross-section a equation was developed and presented in Equation 3.3.

$$a_2 = \frac{L_{spv}}{round(\frac{L_{spv}}{6.5m})} \tag{3.3}$$

The design of the transverse beams in field are presented in Figure 3.40, welded to the vertical stiffeners. The bridge is provided with a continuous diaphragm (i.e. rigid support) and the design is presented in Figure 3.41, covering almost the entire space between the two webs.

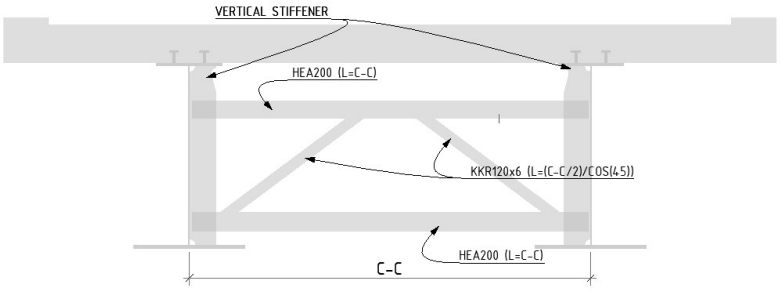

Figure 3.40: *Transverse beams.*

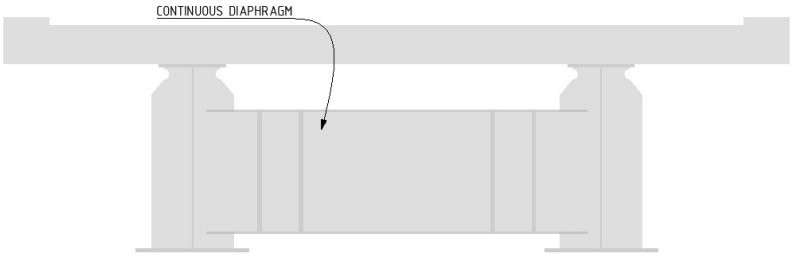

Figure 3.41: *Rigid end support.*

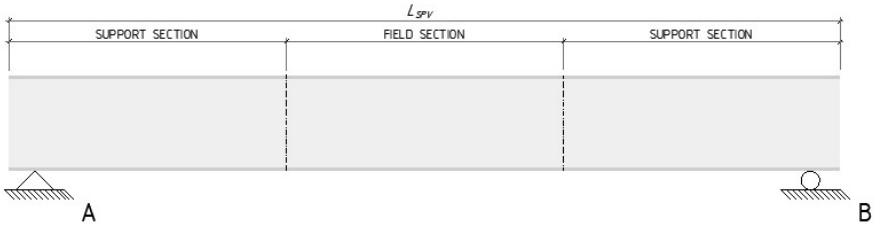

Figure 3.42: *Optimized cross-section of steel cross-sections.*

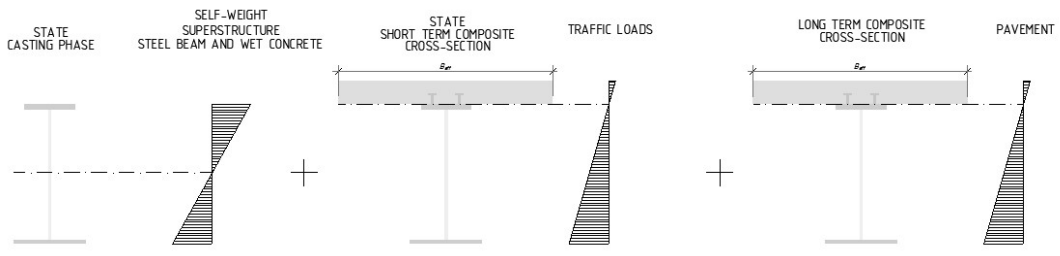

Figure 3.43: *Total stress from moments that cross-sections are optimized for.*

In consideration of LCA, it is important to take into account rolling widths. It is important for the designer to optimize the cross-sections of the beams to use as much material as possible, as steel left over from rolling is usually not reused

without processing. Therefore, minimizing waste is critical. In addition to the beam material, 10 mm is added for each saw cut. The smallest rolling width from SSAB AB is 1750 mm and the largest is 3250 mm. Considering a beam without longitudinal joints as studied in this case. Reasonable rolling lengths are 5 meters, but it is possible to make them up to 23 meters.

3.5.1 Way of bearing

The superstructure consists of two welded steel beams with a concrete slab and associated cantilevers on each side. Full interaction between the steel beams and the concrete slab is considered when the welded studs in the upper flange are cast into the concrete slab.

The steel girders carry the loads in the longitudinal direction with beam action to the supports on each side, and the cantilever carries the loads in the transverse direction.

Permanent loads are distributed equally between both steel beams. While the variable traffic load is distributed according to position and magnitude, in relation to the supporting girders by width, where one girder carries more load than the other. The magnitude of the worst loaded girder is defined by a field factor which is a size ratio based on all applied traffic loads in relation to load lane 1.

To optimize the beams in terms of traffic loads, the worst shear force and moment for load lane 1 were iterated for each one-eighth section using the software Strip Step2 (VERSION PC-05). This calculation was performed for every other meter length from 6 to 40 meters. If the beam is divided at a section other than an one-eighth section, the programming determines the shear force and moment through linear interpolation between the one-eighth sections, thus obtaining all section forces. One-eighth sections with linear interpolation between measured data are considered arbitrarily as the governing load effect for the beams in terms of variable load.

Each beam is therefore designed for the worst shear force and moment, where the programming selects the worst traffic load (between LM1 and Vehicle Loads A-O). The measurement points are located at each one-eighth section with linear interpolation in between. The support beam is designed for the worst shear force with the corresponding moment, while the field beam is designed for the worst field moment with the corresponding shear force, see Figure 3.44, and where the lengths of the beam are determined with Equation 3.1.

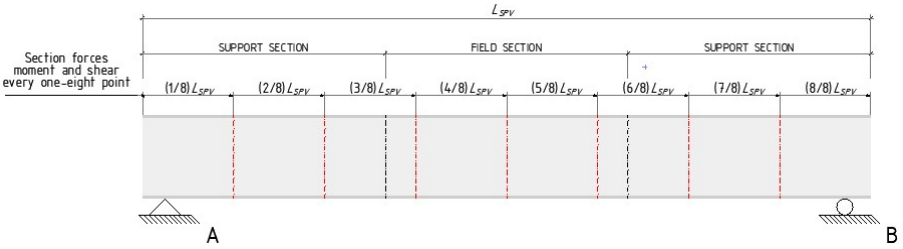

Figure 3.44: *Sections forces derived from every one-eight section.*

The load cases are varying depending on the bridge span length. The load factor changes correspondingly on whether LM1 or A-O Vehicle loads (Transportstyrelsen, 2018) are dominant. If LM1 is dominant for a specific span length, it is calculated according to Figure 3.45. The A-O Vehicle loads (Transportstyrelsen, 2018) have a percentage relationship to the other load lanes and can therefore be calculated according to Figure 3.46, where the loads from Vehicle Model I is used. Since a unique load case is used for fatigue, a load factor is also needed, which is calculated according to Figure 3.47.

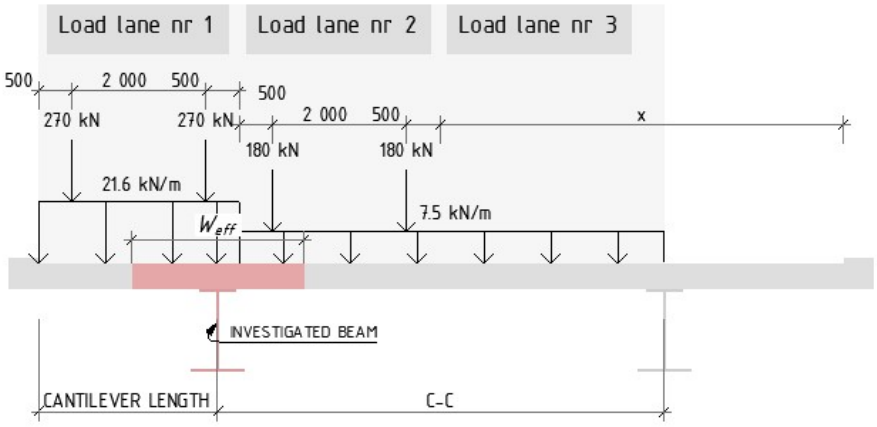

Figure 3.45: *Field factor with LM1.*

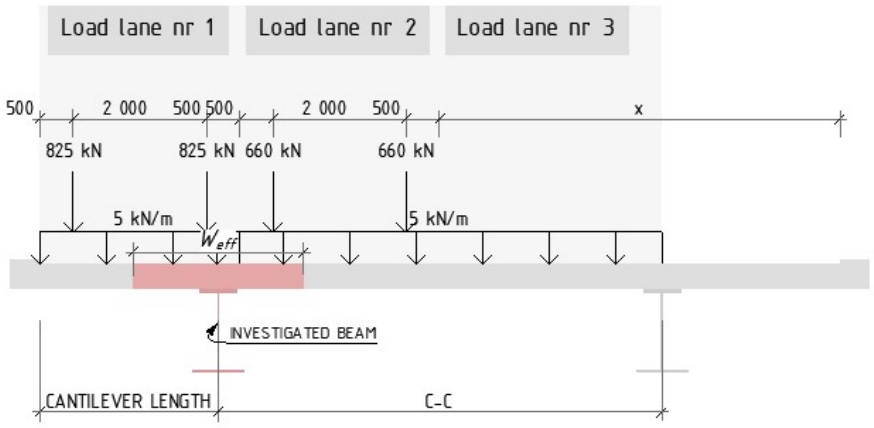

Figure 3.46: *Field factor for Vehicle loads A-O.*

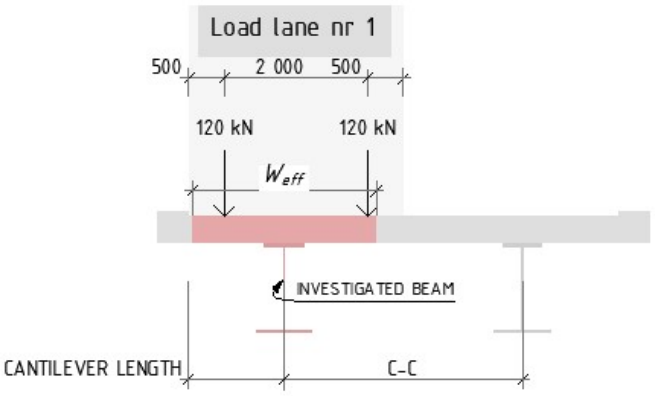

Figure 3.47: *Field factor with fatigue load model 3 (FLM3).*

3.5.1.1 Cross-sections

To simplify calculations, only the load effect and capacity of one beam cross-section is examined. The cross section varies and is loaded with corresponding loads for the current phase.

- Phase 1 (short-term, casting phase): Steel cross section: loaded with the self-weight of the steel beam and wet concrete.
- Phase 2 (short-term): Composite cross section: loaded with variable loads (traffic loads).
- Phase 3 (long-term): Composite cross section loaded with pavement.

In phase 1, during the casting phase, there is no interaction between the concrete and steel cross section as the concrete is still wet and cannot contribute any shear capacity from the bond between the steel beam and concrete. Since the cross section has not achieved full interaction, a part of the cross section will be under compression. When the steel cross section is under compression, the bending behavior of the

cross section is regulated according to (CEN., 2005c). Each part of the cross section is regulated separately, with flanges as outstand flanges and webs as internal compression parts, according to Table 5.2 in (CEN., 2005c). These cross-section classes are based on the cross section's design. Stocky sections are capable of developing their full plastic capacity. More slender sections are capable of developing their full elastic resistance, but parts under compression will buckle after a certain limit. However, very slender sections will buckle elastically, and therefore, the capacity of the cross-section parts must be reduced according to (CEN., 2006) Tables 4.1 and 4.2 as in Figure 3.48.

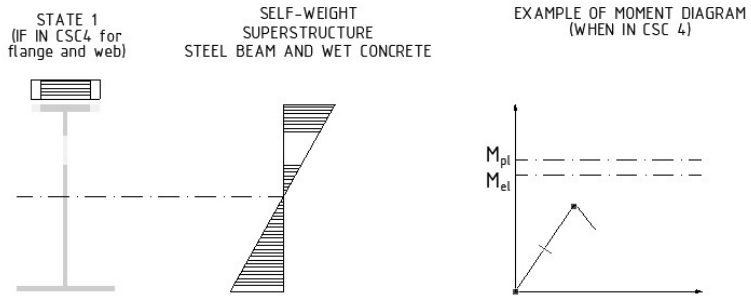

Figure 3.48: *Reduced cross-section in CSC 4.*

In phases 2 and 3, the beam cross section has achieved composite action. Since the weight, size, and stiffness of the concrete relative to the steel are significantly higher, the upper part of the beam will be in compression, but the center of gravity is located significantly higher within an composite cross-section. As a result, only a small portion of the cross-section is under compression, making any potential reduction negligible. The effective concrete flange in phase 2 is regulated according to (CEN., 2005f) Section 5.4.1.2. In the long term, creep and shrinkage are also included.

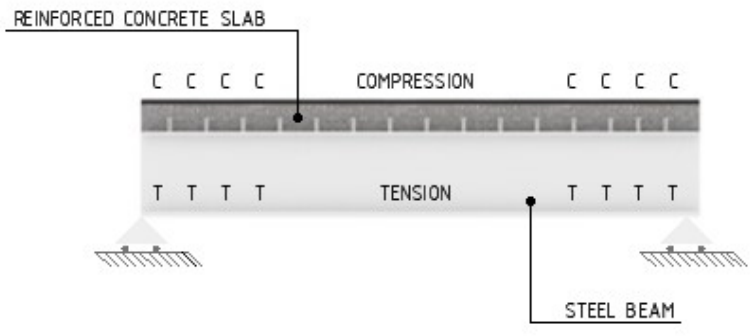

Figure 3.49: *Composite action.*

3.5.2 Reinforcement design of concrete

As previously mentioned, the constant concrete cross-section is based on the sizing of the cantilever in the restraint section. However, the amount of reinforcement is

based on experience and comes from Inhouse Tech AB. The reinforcement used in LCA calculations consists of longitudinal tensile reinforcement with a diameter of 16 mm and a spacing of 120 mm at the top and bottom. Transverse reinforcement has a diameter of 16 mm and a spacing of 100 mm. Figure 3.50 describes a section of the reinforcement amount. For splicing of reinforcement, a factor of 1.2 is used on the total reinforcement amount, which is also based on experience.

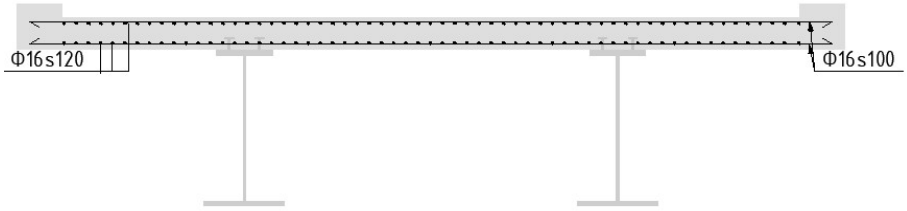

Figure 3.50: *Reinforcement design of concrete.*

3.5.3 Resistance checks in ULS

3.5.3.1 Shear force capacity

The shear force capacity of the web with regard to shear buckling is calculated according to (CEN., 2006) and is presented in Equation 3.4, where the design yield strength of the web f_{yw} and material partial factor γ_{M1} is included.

$$V_{bw.Rd} = \frac{\chi_w \cdot f_{yw} \cdot h_w \cdot t_w}{\sqrt{3} \cdot \gamma_{M1}} \tag{3.4}$$

To decide the χ_w factor, both the slenderness factor λ_w and the shear buckling coefficient k_T need to be decided. The shear buckling coefficient is depending on the ratio between the distance between the vertical stiffener a and the height of the web h_w, and is presented in Equation 3.5 and Equation 3.6.

$$k_\tau = 5.34 + 4 \cdot (\frac{h_w}{a})^2 \qquad \text{if } \frac{a}{h_w} \geq 1 \tag{3.5}$$

$$k_\tau = 4 + 5.34 \cdot (\frac{h_w}{a})^2 \qquad \text{if } \frac{a}{h_w} \leq 1 \tag{3.6}$$

The composite bridge will be designed with transverse stiffeners at supports and intermediate transverse stiffeners and therefore Equation 3.7 is used.

$$\lambda_w = \frac{h_w}{37.4 \cdot t_w \cdot \epsilon \cdot \sqrt{k_\tau}} \tag{3.7}$$

Where ϵ is defined as in Equation 3.8.

$$\epsilon = \sqrt{\frac{235}{f_y}} \tag{3.8}$$

As mentioned before, the bridge will be designed with transverse stiffeners at the supports and is therefore considered to have rigid end posts. With this knowledge

and the material parameter η, which is equal to 1.2 for steel grades below S460 and equal to 1 for steel grades above, the following statements in Equation 3.9 are checked to get the χ_w factor.

$$\begin{aligned} \chi_w &= \eta && \text{if } \lambda_w \leq \frac{0.83}{\eta} \\ \chi_w &= \frac{0.83}{\lambda_w} && \text{if } \frac{0.83}{\eta} < \lambda_w \leq 1.08 \\ \chi_w &= \frac{1.37}{0.7 + \lambda_w} && \text{if } \lambda_w > 1.08 \end{aligned} \tag{3.9}$$

3.5.3.2 Bending stress in flanges

To assess the resistance to bending stress in the girder, three stages are defined. The first stage occurs when the concrete deck has been added but has not yet hardened. At this stage, only the I-girder will carry the load from the self-weight of the steel and concrete, and the parts that are in compression need to be checked against the cross-section classes in (CEN., 2005c). If the compressed part is slender, the effective area needs to be calculated, this leads to less stiffness in the girder.

The second stage is when the permanent load is applied, which includes the coating. The third stage is calculated with the traffic loads. Both stages can be considered to carry the load as a composite structure, with calculations to confirm that only the concrete slab is taking the compression stresses the conclusion can be made that no parts in the girder need to be checked against slenderness.

To find out how much of the width of the concrete slab contributes to the composite stiffness, the effective width is calculated in both the mid-span and at the support according to (CEN., 2005e). When calculating the stresses in the top flange for a composite structure it's necessary to transform the concrete slab to one fictive steel flange. For the short-term load in this case the traffic load, an effective modular ratio is calculated to transform the concrete slab area into a fictive steel cross-section and its calculated by dividing the elastic modulus for steel by the elastic modulus for concrete, see Equation 3.10.

$$\alpha_{eff} = \frac{E_s}{E_{cm}} \tag{3.10}$$

For the permanent load the long term effect creep is considered with the creep coefficeint $\phi(\infty, t_0)$, and is included in the calculation of the effective modulus as in Equation 3.11.

$$\alpha_{eff} = \frac{E_s \cdot (1 + \phi(\infty, t_0))}{E_{cm}} \tag{3.11}$$

The stresses in the top flange and bottom flange are summarized for the steps and are checked against the design yield strength of the steel see Equation 3.12.

$$\sigma_{tot.top} = \sigma_{short.top} + \sigma_{perm.top} + \sigma_{pouring.top} \leq f_{yd} \tag{3.12}$$

3.5.3.3 Lateral torsional buckling during pouring concrete

Lateral torsional buckling (LTB) is a failure mode that can occur in girders subjected to vertical load. LTB happens when the girder twists out of its plane under bending loads, which can lead to a sudden failure.

During the pouring of the concrete, the concrete slab is in a liquid state and does not have any significant strength to resist bending. This means that the steel girders are subjected to significant bending loads due to the weight of the wet concrete. As the concrete hardens and gains strength, it provides resistance to bending, but during the pouring phase, the steel girders are carrying most of the load.

If the steel girders are not designed to resist the bending loads during the pouring phase, LTB can occur. This is because the bending loads can cause the steel girders to twist out of their plane, which can lead to a sudden failure. Therefore, it is essential to check for LTB during the pouring phase to ensure that the steel girders can safely resist the bending loads until the concrete hardens and provides additional support.

To reduce the magnitude of the load, the pouring of the concrete is divided into two phases see Figure 3.51.

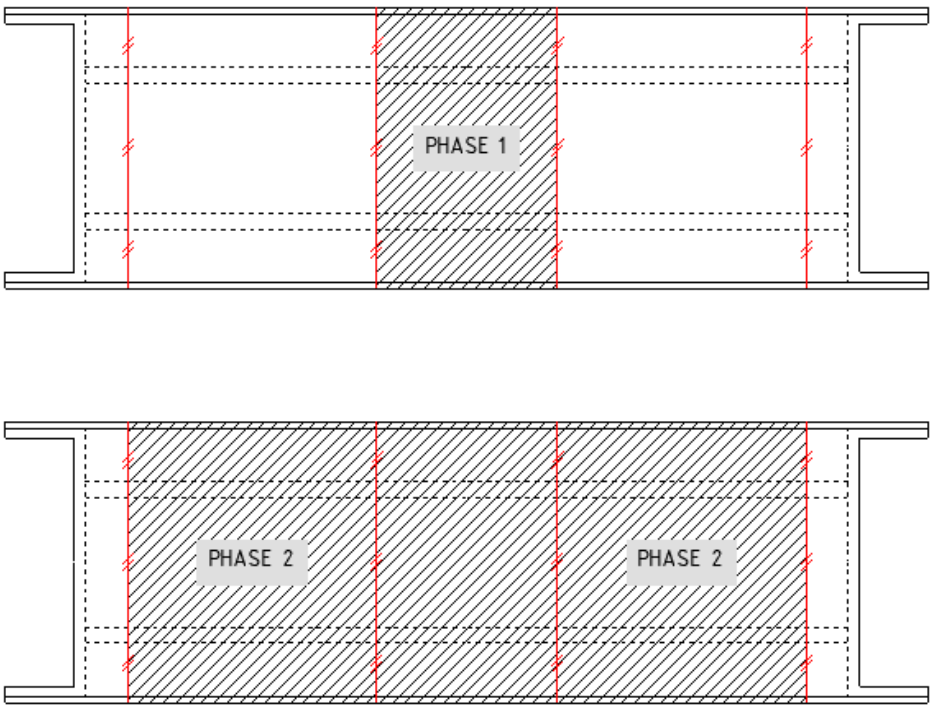

Figure 3.51: *Concrete pouring phases.*

The first phase is set to 60 % of the total self-weight of the concrete and the second phase starts when the concrete has hardened in phase 1.

The LTB resistance of the I-girder is calculated according to (CEN., 2005c) and is defined in Equation 3.13, where the elastic section modulus W_{el} and the material parameter γ_{M1} is included.

$$M_{b.Rd} = \chi_{LT} \cdot W_{el} \cdot \frac{f_{yd}}{\gamma_{M1}} \geq M_{Ed} \tag{3.13}$$

The reduction factor χ_{LT} is calculated with the slenderness parameter λ_{LT} and the Φ_{LT} factor which is depending on the cross-section and manufacturing method and is described in Equation 3.14.

$$\chi_{LT} = min(\frac{1}{\Phi_{LT} + \sqrt{\Phi_{LT}^2 - \lambda_{LT}^2}}, 1) \tag{3.14}$$

3.5.3.4 Studs

The studs have a diameter of 22 mm and height of 350 mm and are arranged in pairs with a center distance of 200 mm, as in Figure 3.52. The capacity is calculated according to EN 1994-2 Part 6.6.3.1 (CEN., 2005f). At the supports, the edge distance is designed based on ULS load combination, and in the field with regard to fatigue load combination. The edge distance is then linearly reduced until the point where the edge distance for fatigue is reached. This is part of the optimization process, as the number of studs can be significantly limited if they are not only designed for the worst case scenario. In addition to being a saving in terms of LCA, it also saves welding hours.

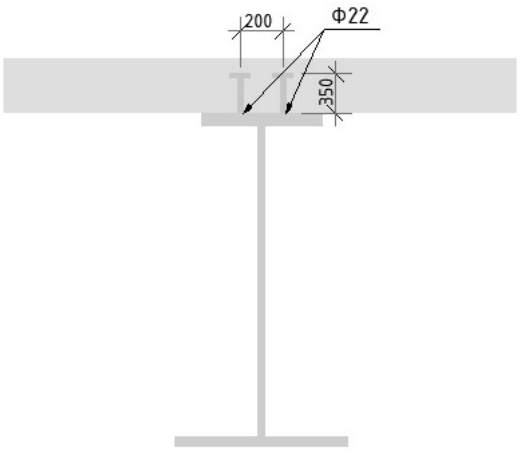

Figure 3.52: *Studs.*

In Figure 3.53 an example of the decreasing number of studs along the bridge is presented, where the x-axis is the length of beam from the support and y-axis describes the required number of studs per meter.

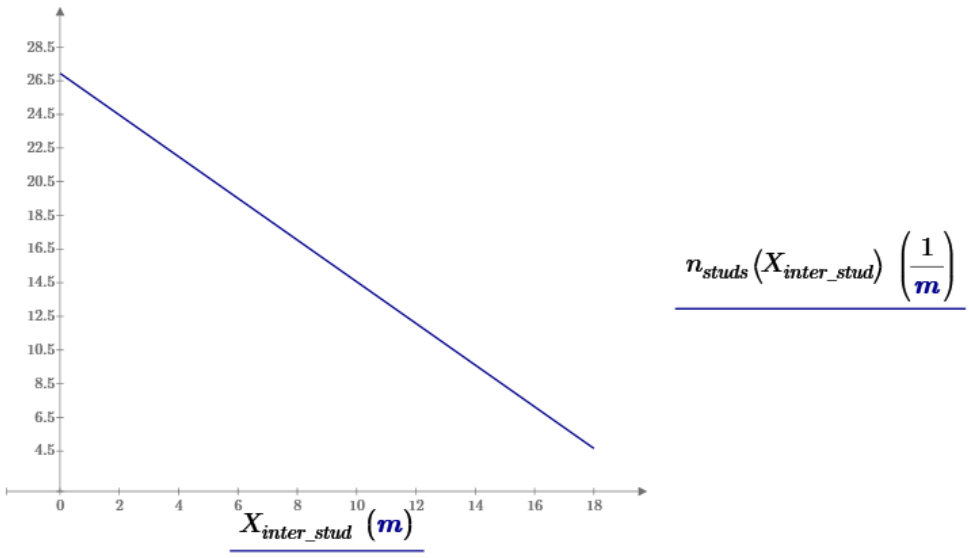

Figure 3.53: *Linear decreasing number of studs per meter for a 36-meter long bridge.*

3.5.4 Deformation checks in SLS

Deformation checks in SLS are carried out in frequent load combination, and the stiffness of the composite cross-section is calculated. The effective width of one girder is determined, and the concrete slab is transformed into a fictitious steel flange using a factor calculated based on the ratio of the elastic modulus of steel and concrete, see Equation 3.6.

As mentioned in the previous chapter the vertical deformation should be controlled with only variable loads, and both the maximum deflection in the span and at the cantilever. For the deflection in the span elementary case for a simply supported beam is used and controlled against $L_{spv}/400$. The deflection in the cantilever is controlled with calculating the support rotations and should be less than or equal to 5 mm.

3.5.5 Fatigue verification

From an LCA perspective, it is important to consider the service life of the bridge, a longer service life gives a higher benefit per emission. When dimensioning for time, fatigue must be taken into account. Fatigue occurs with repeated loads and can lead to fracture. According to (Trafikverket, 2022), the service life should be set to at least 80 years.

Fatigue Load Model 3 (FLM3) is simulated as a single vehicle with four axles with 120 kN load for each axle, the vehicle geometry is presented in Figure 3.54.

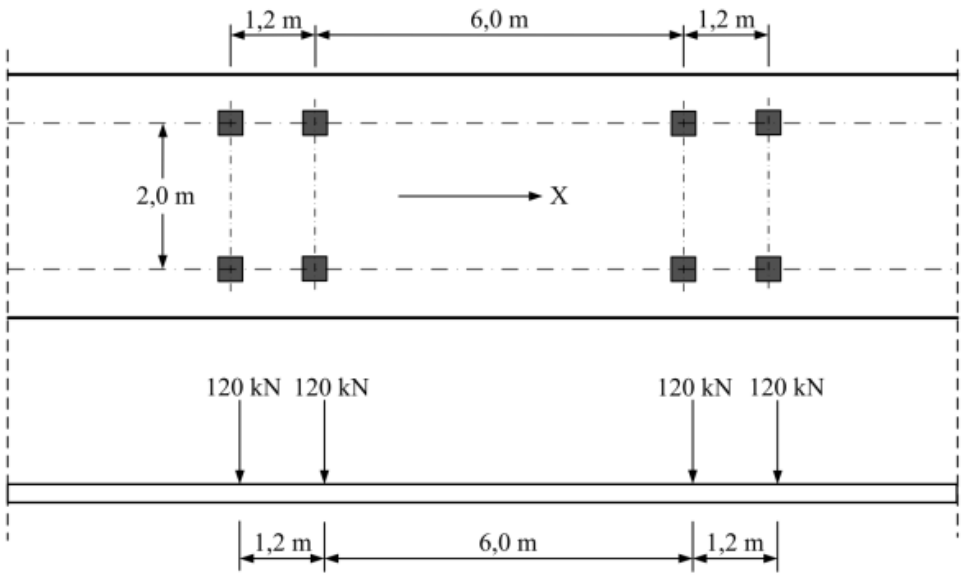

Figure 3.54: *FLM3 according to(CEN., 2003).*

The FLM3 is utilized to confirm the fatigue life of the examined details by computing the max and min stresses caused by the load model's longitudinal and transversal location. The aim of this load model is to use the simplified *lambda* method to ensure that the stress range computed is not greater than the fatigue strength of the examined detail. However, the method is sufficiently accurate for road bridges with spans exceeding 10 meters, as it tends to provide conservative results for shorter spans according to (Al-Emrani & Aygül, 2014).

The purpose of the simplified *lambda* method is to convert fatigue verifications using λ-coefficients into a conventional fatigue resistance control. The λ factor is calculated with Equation 3.15.

$$\lambda = \lambda_1 \cdot \lambda_2 \cdot \lambda_3 \cdot \lambda_4 \leq \lambda_{max} \tag{3.15}$$

The factors are taking the following parameters into account and can be found in (CEN., 2009).

- $\lambda_1 \rightarrow$ Length of the span and structure type
- $\lambda_2 \rightarrow$ Taking the the traffic volume into account
- $\lambda_3 \rightarrow$ Time factor regarding the design life time of the bridge
- $\lambda_4 \rightarrow$ Taking the number of traffic lanes into account
- $\lambda_{max} \rightarrow$ The maximum damage equivalent factor

With the λ factor calculated the fatigue verification for each detail can be determined with Equation 3.16.

$$\gamma_{Ff} \cdot \lambda \cdot \Phi_2 \cdot \sigma_{FLM} \leq \frac{\Delta\sigma_C}{\lambda_{max}} \tag{3.16}$$

where the parameters are:

- $\gamma_{Ff} \rightarrow$ Partial safety factor for fatigue loading
- $\Phi_2 \rightarrow$ Dynamic factor
- $\sigma_{FLM} \rightarrow$ Stress range due to the fatigue load model
- $\Delta\sigma_C \rightarrow$ Responding fatigue resistance at 2 milion cycles for the studied detail

In this study, the fatigue capacity of the weldings is neglected due to it being more of a cost issue than an LCA question. The details that are checked in the steel girder are presented in Figure 3.55 and the detail category with belonging fatigue resistance is presented in Table 3.1.

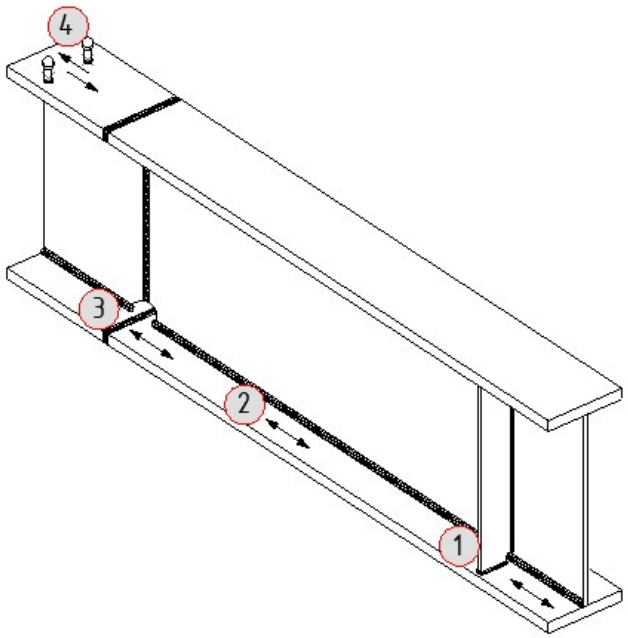

Figure 3.55: *Fatigue details.*

Table 3.2: Studied fatigue details.

Description	**Responding table and detail number (CEN., 2005d)**	**Fatigue resistance at 2 million cycle**
1) Normal stress in the connection of the vertical stiffener to the lower flange in mid-span.	Table 8.4, Detail number 7	$\Delta\sigma_C = 80$ MPa
2) Normal stress at girder splice	Table 8.2, Detail number 4	$\Delta\sigma_C = 112$ MPa
3) Normal stress in the rat-hole detail at the girder splice	Table 8.2, Detail number 9	$\Delta\sigma_C = 71$ MPa
4) Shear stress capacity for studs at mid-span	Table 8.5, Detail number 10	$\Delta\tau_C = 90$ MPa

3.5.6 Input data MathCAD tool

The span lengths that are investigated for this bridge type are set to 20-40 meter, as lower span lengths aren't feasible for this construction type, and the bridge width 6-12 meter.

For steel-concrete composite bridges there are many parameters for the input and to reduce the complicity of the iteration some of them are predefined with equations developed from studying real bridges. The Height of the I-girder is approximated to be 5 % of the span length of the bridge, and the height of the web is calculated to the total height of the girder subtracted with the thickness of the flanges. The I-girder consists of two cross-sections, one at the supports for mainly resist the shear force with thicker web and thinner flanges, the cross-section at the mid-span is designed to resist the bending moment mainly in the flanges, also the fatigue will be governing for the lower flange.

The iteration process begins with inserting the input consisting of span length, the width of the bridge, pavement thickness, and height of the I-girder, also a guess of the dimensions of the width of the web and flange dimensions. The length of the console is defined regarding the width of the bridge. To iterate effectively a flowchart is developed and is presented in Figure 3.56.

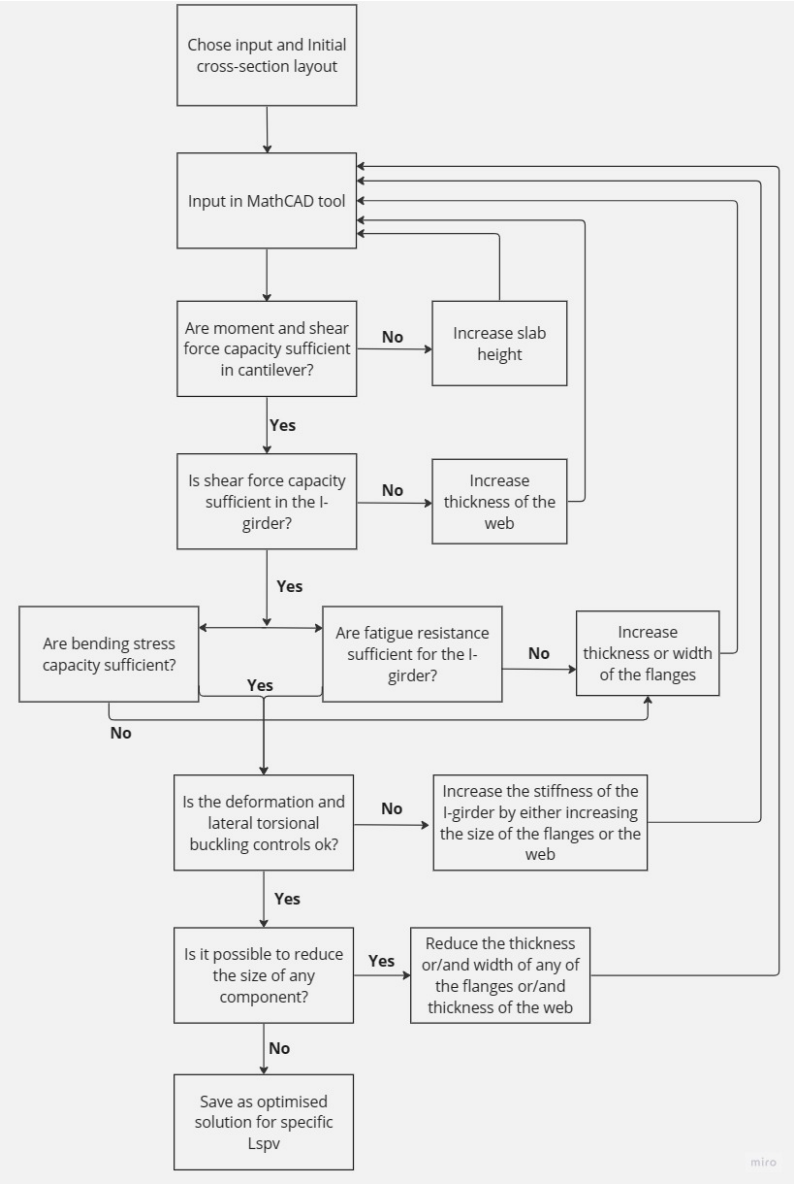

Figure 3.56: *Iteration method for steel-concrete composite bridge.*

To reduce the iteration time, minimum limits on the change of the I-girder's cross-section have been implemented. The width of the flanges is allowed to change by a maximum of 50 mm, and the thickness by 5 mm. The minimum change for the web thickness is set to 1 mm.

4
Results

In general, it can be observed that slab bridges are more suitable for shorter spans when considering CO_2-equivalents. However, the choice of bridge type for longer spans varies and is highly dependent on the width of the carriageway.

In the upcoming chapter, the results for each bridge type and carriageway width will be discussed, highlighting the key factors influencing the design. Subsequently, a comparison between the different bridge types for each carriageway width will be presented when it comes to CO_2-equivalents.

4.1 Girder bridge

Overall, for carriage way widths for girder bridges, the total equivalent carbon dioxide content increases with increased span length. The bridge, which has a carriageway width of 6 meters, experiences several decisive load cases: compression in bottom of cross-section in quasi-permanent load combination for short-term response, tension bottom of cross-section in frequent traffic load combination, and vertical displacement of the end cantilevers. This results in an inconsistent curve (see Figure 4.1, $b = 6$ m), which changes slope at three points. However, the same load case (tension in bottom of the cross-section in frequent load combination) dominates for all lengths of 9-meter and 12-meter carriageway widths, resulting in a half parabola, where the 12-meter carriageway width has a steeper increase than the 9-meter carriageway width (see Figure 4.1, $b = 9$ m and $b = 12$).

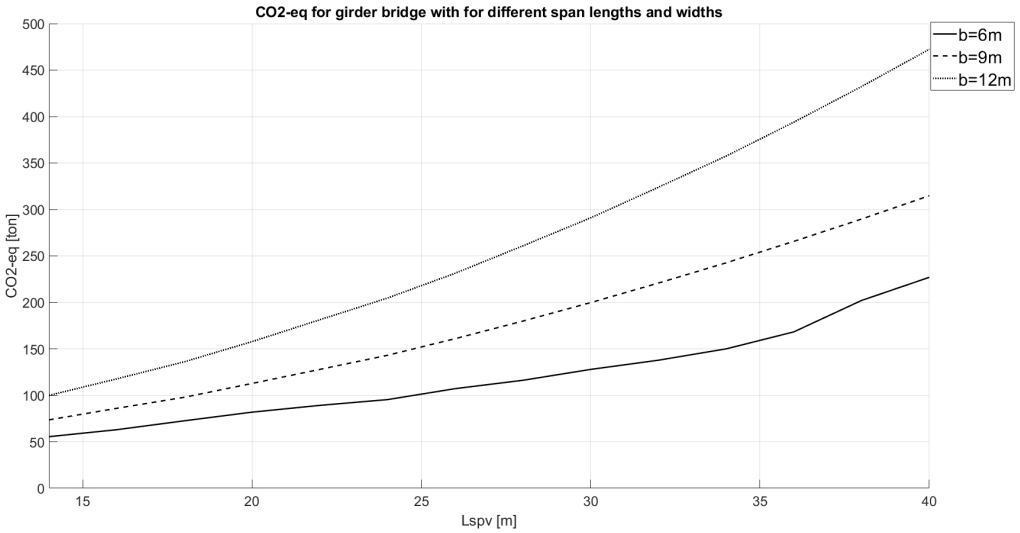

Figure 4.1: *Results girder bridges.*

4.1.1 6 m carriageway width

The maximum allowed beam height ($L_{spv}/20$) applies consistently to all span lengths tested for (Table 4.1, row 2). For 14-meter and 16-meter span length L_{spv}, compression in bottom of the cross-section in mid span under the quasi-permanent load combination is the decisive. For the 18-meter span length, the frequent load combination is decisive. This required an increase in the number of cables (see Table 4.1). For the 20-meter girder bridge, once again, compression in bottom of the cross-section from the quasi-permanent load combination is decisive for design, necessitating an increased beam width (self-weight).

From 24 meters to 34 meters of span length, the deflection of the end cantilevers in SLS is the dominant load case. At a 24-meter L_{spv}, it is noteworthy that it is possible to reduce the number of cables by 1 cable.

For span lengths ranging from 36 meters to 40 meters, tension in bottom mid span under the frequent load combination is decisive. Despite being the same load combination, the point between 36-38 meters shows a noticeable deviation in the increase of CO_2-eq compared to 38-40 meters. This is because the beam increases significantly in width from 36-38 meters (from 2.2 m to 2.8 meters) compared to 38-40 meters (2.8 to 3 meters). The beam width was increased because the maximum number of cables needed to be increased (to achieve additional compression from moments at the bottom in mid span). As the moment increases exponentially with the length of the beam, the increased self-weight has a greater negative impact than the positive impact of an additional cable. This resulted in a 2.8-meter-wide beam and 12 tendons. Between 38-40 meters, it was sufficient to increase the beam width by 0.2 meters and add another tendon.

Table 4.1: Final input for MathCAD tool girder bridge, at 6 m carriageway width.

L_{spv} [m]	h [m]	b [m]	L_{cant} [m]	$n_{tendons}$	CO_2-eq tot [tons]
14	0.7	3.6	1.2	7	55.5
16	0.8	3.4	1.3	7	63.0
18	0.9	3.4	1.3	8	72.6
20	1.0	3.2	1.4	8	81.9
22	1.1	2.8	1.6	8	89.2
24	1.2	2.4	1.8	7	95.4
26	1.3	2.4	1.8	8	107.2
28	1.4	2.2	1.9	8	116.2
30	1.5	2.2	1.9	8	127.9
32	1.6	2	2	9	137.8
34	1.7	2	2	9	150.0
36	1.8	2.2	1.9	10	168.3
38	1.9	2.8	1.6	12	202.1
40	2.0	3	1.5	13	227.0

4.1.2 9 m carriageway width

For length bridges ranging from 14 to 40 meters, the tension at the bottom of cross-section in span (under frequent load combination) is decisive. It is also possible to have a maximum cantilever length of 2.5 meters on both sides of the main beam for all lengths, which means the minimum possible width **b = 4 meters** of the beam (Table 4.2 row nr 3). Increasing the number of cables is the main method to accommodate this requirement. It is worth noting that the number of cables can be reduced for a 24-meter beam (Table 4.2).

Table 4.2: Final input for MathCAD tool girder bridge, at 9 m carriageway width.

L_{spv} [m]	h [m]	b [m]	L_{cant} [m]	$n_{tendons}$	CO_2-eq tot [tons]
14	0.7	4	2.5	8	73.6
16	0.8	4	2.5	9	86.0
18	0.9	4	2.5	9	97.9
20	1.0	4	2.5	10	112.8
22	1.1	4	2.5	10	127.9
24	1.2	4	2.5	9	143.1
26	1.3	4	2.5	10	161.0
28	1.4	4	2.5	11	179.9
30	1.5	4	2.5	12	199.8
32	1.6	4	2.5	13	220.8
34	1.7	4	2.5	14	242.6
36	1.8	4	2.5	15	265.7
38	1.9	4	2.5	16	289.7
40	2.0	4	2.5	17	314.8

4.1.3 12 m carriageway width

The maximum beam height($L_{spv}/20$) was iterated for all span lengths studied. For all span length ranging from 14 to 40 meters, tension at the bottom of the cross-section (frequent load combination) is decisive. For all lengths, it is also possible to have a maximum cantilever length of 2.5 meters, which corresponds to the minimum possible width of the beam. Increasing the number of tendons resolves the control issue with the frequent traffic load combination (Table 4.3). What is noteworthy is that it is possible to reduce the number of cables with 1 tendon cable 24-meter beam bridge in comparison to 22 meter.

Table 4.3: Final input for MathCAD tool girder bridge, at 12 m carriageway width.

L_{spv} **[m]**	**h [m]**	**b [m]**	L_{cant} **[m]**	$n_{tendons}$	CO_2**-eq tot [tons]**
14	0.7	7	2.5	10	99.9
16	0.8	7	2.5	11	117.7
18	0.9	7	2.5	12	136.1
20	1.0	7	2.5	13	157.8
22	1.1	7	2.5	14	181.3
24	1.2	7	2.5	13	204.7
26	1.3	7	2.5	14	231.4
28	1.4	7	2.5	16	260.9
30	1.5	7	2.5	17	291.0
32	1.6	7	2.5	19	323.9
34	1.7	7	2.5	20	357.5
36	1.8	7	2.5	22	394.0
38	1.9	7	2.5	24	432.3
40	2.0	7	2.5	25	472.4

4.2 Steel concrete composite bridge

The steel-concrete composite bridge total equivalent carbon dioxide content increases with increased span length and width. As presented in Figure 4.2, the curve increases almost linearly but with some deviations.

The deviations have several reasons, for each increasing span length the cross-section of the I-girder may be updated if required according to the controls in SLS and ULS. With predefined minimum changes of the I-girders, these increasing changes lead to a low-efficiency ratio for the control that is mainly affected by the detail that is changed, and at next span length check it may lead to no changes in the cross-section.

The deviations are also affected by the number of vertical stiffeners and transverse beams, as the amount increases with increasing span lengths but not for each step as described in Equations 3.1 and 3.2.

In the following sections the general input and the CO_2-eq for each span length, and the chosen cross sections are presented in tables for each span length with the belonging bridge width.

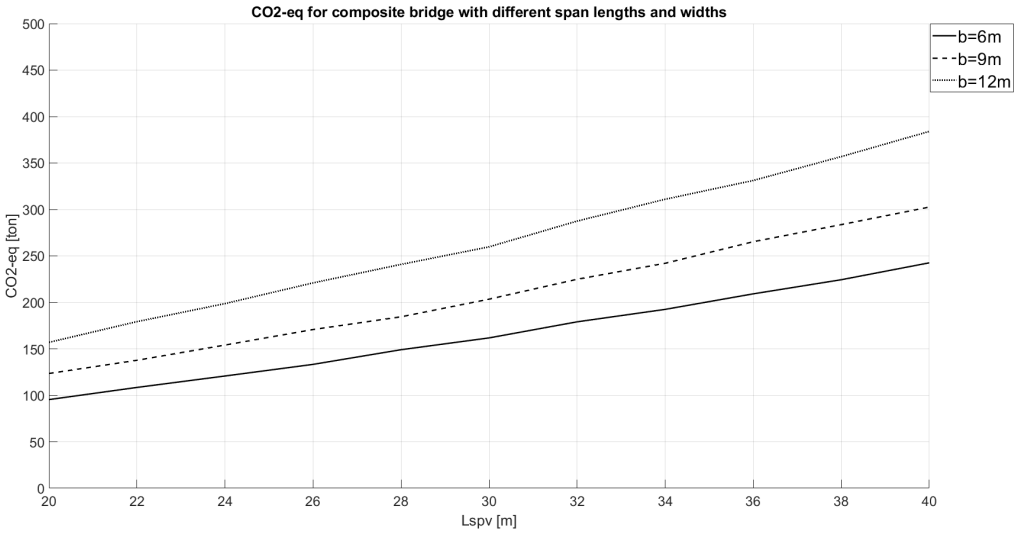

Figure 4.2: *Different widths of composite bridges.*

The results have been taken out with the fatigue load amount of heavy lorries to correspond to a main road with low amount of heavy lorries according to (CEN., 2009).

The notations of the detail dimensions used in Tables 4.4-4.6 are presented in Figure 4.3.

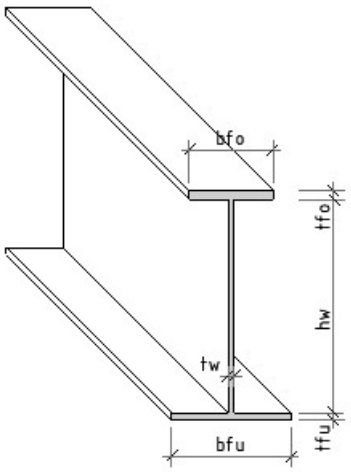

Figure 4.3: *Notions for I-girder details parameter*

4.2.1 6 m carriage width

Table 4.4: General input and CO_2-eq for steel concrete composite bridge with 6m width.

L_{spv} [m]	**Cantilever length [m]**	**Concrete slab height [mm]**	**Length of girder placed closer to support [m]**	CO_2**-eq [ton]**
20	1.5	240	3	95.4
22	1.5	240	4	108.5
24	1.5	240	4	120.8
26	1.5	240	4	133.3
28	1.5	240	5	149.1
30	1.5	240	6	161.8
32	1.5	240	7	179.1
34	1.5	240	8	192.5
36	1.5	240	9	209.2
38	1.5	240	10	224.4
40	1.5	240	11	242.6

Table 4.5: Cross section data for I-girder in mid span.

L_{spv} [m]	h_w [mm]	t_w [mm]	b_{fu} [mm]	t_{fu} [mm]	b_{fo} [mm]	t_{fo} [mm]
20	930	10	800	55	300	15
22	1025	10	800	60	300	15
24	1125	11	800	60	300	15
26	1225	11	850	60	300	15
28	1320	11	900	60	300	20
30	1420	11	900	60	300	20
32	1515	11	900	65	350	20
34	1615	11	900	65	350	20
36	1710	11	900	65	350	25
38	1810	11	900	65	350	25
40	1905	11	900	65	350	30

Table 4.6: Cross section data for I-girder closer to support.

L_{spv} [m]	h_w [mm]	t_w [mm]	b_{fu} [mm]	t_{fu} [mm]	b_{fo} [mm]	t_{fo} [mm]
20	945	11	650	40	300	15
22	1040	11	700	45	300	15
24	1145	12	750	40	300	15
26	1240	12	600	45	300	15
28	1330	12	600	55	300	15
30	1430	12	650	55	300	15
32	1520	12	600	65	300	15
34	1620	12	650	65	300	15
36	1715	12	650	70	300	15
38	1815	13	650	70	300	15
40	1905	13	650	75	350	20

4.2.2 9 m carriage width

Table 4.7: General input and CO_2-eq for steel concrete composite bridge with 9 meter width.

L_{spv} [m]	Cantilever length [m]	Concrete slab height [mm]	Length of girder placed closer to support [m]	CO_2-eq [ton]
20	2	280	3	123.5
22	2	280	4	137.7
24	2	280	4	154.1
26	2	280	4	170.8
28	2	280	5	184.5
30	2	280	6	203.5
32	2	280	7	224.9
34	2	280	8	242.1
36	2	280	9	265.3
38	2	280	10	283.7
40	2	280	11	302.6

Table 4.8: Cross section data for I-girder in mid span width 9 meter.

L_{spv} [m]	h_w [mm]	t_w [mm]	b_{fu} [mm]	t_{fu} [mm]	b_{fo} [mm]	t_{fo} [mm]
20	930	13	850	55	300	15
22	1025	13	850	55	300	20
24	1125	13	900	55	300	20
26	1215	14	850	60	300	25
28	1315	14	850	60	300	25
30	1410	14	850	60	300	30
32	1505	14	900	60	350	30
34	1615	15	900	60	400	25
36	1700	15	900	65	350	35
38	1800	15	900	65	350	35
40	1895	15	900	65	350	40

Table 4.9: Cross section data for I-girder closer to support width 9 meter.

L_{spv} [m]	h_w [mm]	t_w [mm]	b_{fu} [mm]	t_{fu} [mm]	b_{fo} [mm]	t_{fo} [mm]
20	940	14	600	45	300	15
22	1035	15	650	50	300	15
24	1130	15	600	50	300	20
26	1235	15	650	45	300	20
28	1330	15	650	50	300	20
30	1420	15	650	60	300	20
32	1515	15	700	65	300	20
34	1620	16	750	60	350	20
36	1710	16	700	65	300	25
38	1810	16	750	65	300	30
40	1905	16	750	65	300	30

4.2.3 12 m carriage width

Table 4.10: General input and CO_2-eq for steel concrete composite bridge with 12 meter width.

L_{spv} [m]	Cantilever length [m]	Concrete slab height [mm]	Length of girder placed closer to support [m]	CO_2-eq [ton]
20	2.5	360	3	157
22	2.5	360	3	179.3
24	2.5	360	3	198.3
26	2.5	360	4	221
28	2.5	360	5	240.9
30	2.5	360	6	259.8
32	2.5	360	7	287.5
34	2.5	360	8	311
36	2.5	360	9	331.2
38	2.5	360	10	356.9
40	2.5	360	11	384

Table 4.11: Cross section data for I-girder in mid span width 12 meter.

L_{spv} [m]	h_w [mm]	t_w [mm]	b_{fu} [mm]	t_{fu} [mm]	b_{fo} [mm]	t_{fo} [mm]
20	920	15	850	50	300	30
22	1015	15	850	55	400	30
24	1115	16	900	55	350	30
26	1210	16	850	60	450	30
28	1310	16	850	60	550	30
30	1410	16	850	60	550	30
32	1495	17	900	60	400	45
34	1600	16	900	65	600	35
36	1690	17	900	60	400	50
38	1795	16	900	65	600	40
40	1870	17	900	65	400	65

Table 4.12: Cross section data for I-girder closer to support width 12 meter.

L_{spv} [m]	h_w [mm]	t_w [mm]	b_{fu} [mm]	t_{fu} [mm]	b_{fo} [mm]	t_{fo} [mm]
20	945	16	800	30	300	25
22	1040	16	800	35	350	25
24	1150	17	800	30	300	20
26	1235	17	800	40	400	25
28	1335	17	850	40	450	25
30	1435	17	850	40	450	25
32	1510	18	800	50	350	40
34	1625	18	900	45	450	30
36	1705	18	800	55	350	40
38	1820	18	900	50	450	30
40	1895	18	800	55	400	50

4.3 Slab bridge

The results are shown in Figure 4.4, all the widths have the same pattern where the deflection at the cantilever is dominant up to around 20-22 meters and thereafter the bending moment. This can be explained by the maximum amount of tension reinforcement layers is achieved at that stage and the only way to increase the stiffness is to add height to the slab, this leads to more concrete being needed and the CO_2-eq increases more per meter.

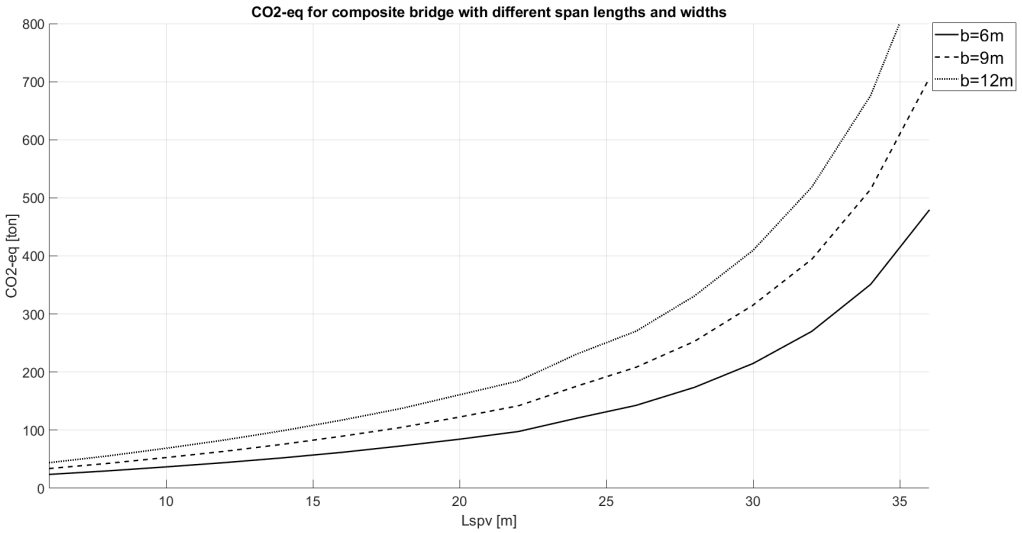

Figure 4.4: *Different widths of slab bridges.*

The tables in the following sections show that the increasing width of the bridge doesn't affect the slab height or the needed amount of tension reinforcement, this can be explained by the assumptions that the load is carried in one-meter width strips and the total load per strip is the same for all widths.

4.3.1 6 meter carriage width

Table 4.13: Input for slab bridge and CO_2-eq for 6 meter width.

L_{spv} [m]	Height slab [mm]	Layer of tension reinforcement	CO_2-eq [ton]
6	350	1	23.8
8	430	2	29.8
10	510	2	36.2
12	580	2	44.2
14	650	2	52.5
16	710	3	61.9
18	780	4	72.8
20	840	4	84.5
22	910	4	97.7
24	1090	4	120.8
26	1230	4	142.6
28	1450	4	173.8
30	1740	4	215
32	2130	4	270.3
34	2700	4	351
36	3610	4	479

4.3.2 9 meter carriage width

Table 4.14: Input for slab bridge and CO_2-eq for 9 meter width.

L_{spv} [m]	Height slab [mm]	Layer of tension reinforcement	CO_2-eq [ton]
6	350	1	33.9
8	430	2	42.8
10	510	2	52.9
12	580	2	63.7
14	650	2	75.9
16	710	3	89.7
18	780	4	104.7
20	840	4	122.7
22	910	4	142
24	1090	4	176
26	1230	4	208.2
28	1440	4	253
30	1740	4	315.5
32	2110	4	394.5
34	2680	4	514.7
36	3590	4	705.9

4.3.3 12 meter carriage width

Table 4.15: Input for slab bridge and CO_2-eq for 12 meter width.

L_{spv} [m]	Height slab [mm]	Layer of tension reinforcement	CO_2-eq [ton]
6	350	1	44
8	430	2	55.6
10	510	2	68.9
12	580	2	83.2
14	650	2	99.3
16	710	3	117.5
18	780	4	137.3
20	840	4	161
22	900	4	184.8
24	1090	4	231.3
26	1210	4	270.3
28	1430	4	331.2
30	1710	4	409.9
32	2100	4	518.8
34	2660	4	676.2
36	3560	4	928

4.4 Comparison bridge types

The comparison between bridge types for each carriageway width is of particular interest as it reveals the most advantageous bridge type for specific span lengths when it comes to CO_2-equivalents.

In the upcoming subchapter the results will be commented when comparing the bridge types and their respective CO_2-equivalents.

4.4.1 6 meter carriageway width

At a 6-meter carriageway width, there are two bridges that dominate in terms of the lowest carbon footprint: the slab bridge and the prestressed girder bridge.

For the shorter span lengths ranging from 6 to 16 meters, the slab bridge has the lowest CO_2-equivalents. The transition point from the slab bridge to the prestressed girder bridge is at 16 to 18 meters of span length.

From 18 to 40 meters with a 6-meter wide carriageway, the most advantageous option in terms of CO_2-equivalents is a prestressed girder bridge.

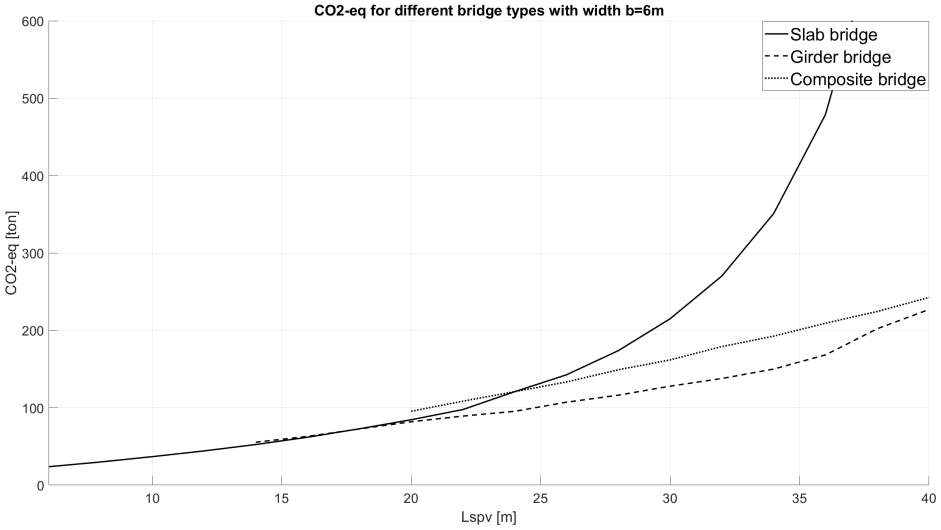

Figure 4.5: *Comparison carriageway width b=6 meter.*

Table 4.16: Comparison between bridges CO_2-eq, at 6 meter carriageway width.

L_{spv} [m]	Slab bridge CO_2-eq[tons]	Girder bridge CO_2-eq[tons]	Steel-concrete comp. CO_2-eq[tons]
6	**23.8**	-	-
8	**29.9**	-	-
10	**36.8**	-	-
12	**44.2**	-	-
14	**52.5**	55.5	-
16	**61.9**	63	-
18	72.8	**72.6**	-
20	84.5	**81.9**	95.4
22	97.7	**89.2**	108.5
24	120.8	**95.4**	120.8
26	142.6	**107.2**	133.3
28	173.8	**116.2**	149.1
30	215.0	**127.9**	161.8
32	270.3	**137.8**	179.1
34	351.0	**150.0**	192.5
36	479.0	**168.3**	209.2
38	-	**202.1**	224.4
40	-	**227.0**	242.6

4.4.2 9 meter carriageway width

For a 9-meter wide carriageway, all three types of bridges dominate at different span lengths in terms of the lowest carbon footprint. The lower span lengths are dominated by the slab bridge, the mid-span by the prestressed girder bridge, and the

upper span by the steel-concrete composite bridge.

For the lower spans ranging from 6 to 12 meters, the slab bridge has the lowest total CO_2-eq. The transition point from the slab bridge to the girder bridge occurs at a span length of 12 to 14 meters.

For span lengths from 14 meters to 32 meters, the prestressed girder bridge is the most advantageous option in terms of the lowest CO_2-eq among the three bridges. The transition to the steel-concrete composite bridge occurs at a span length of 32 to 34 meters.

From 34 to 40 meters span length, the steel-concrete composite bridge has the lowest carbon footprint among the 9-meter wide carriageway bridges.

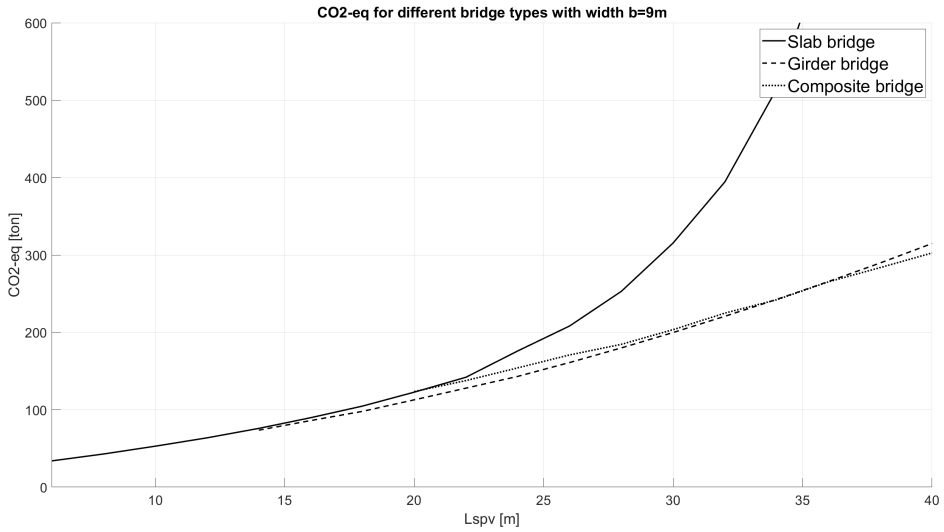

Figure 4.6: *Comparison carriageway width b=9m.*

Table 4.17: Comparison between bridges CO_2-eq, at 9 meter carriageway width.

L_{spv} [m]	Slab bridge CO_2-eq[tons]	Girder bridge CO_2-eq[tons]	Steel-concrete comp. CO_2-eq[tons]
6	**33.9**	-	-
8	**42.8**	-	-
10	**52.9**	-	-
12	**63.7**	-	-
14	75.9	**73.6**	-
16	89.7	**86.0**	-
18	104.7	**97.9**	-
20	122.7	**112.8**	123.5
22	142.0	**127.9**	137.7
24	176.0	**143.1**	154.1
26	208.2	**161**	170.8
28	253.0	**179.9**	184.5
30	315.5	**199.8**	203.5
32	394.5	**220.8**	224.9
34	514.7	242.6	**242.1**
36	705.9	265.7	**265.3**
38	-	289.7	**283.7**
40	-	314.8	**302.6**

4.4.3 12 m carriageway width

For a 12-meter carriageway width, the dominant bridge types in terms of the lowest carbon footprint are primarily the slab bridge and the steel-concrete composite bridges, with the exception of one span length where the prestressed girder bridge is dominant.

For the lower span lengths ranging from 6 meters to 16 meters, the slab bridge is the most advantageous choice and has the lowest CO_2-eq among the three bridge types. At 16 to 18 meters, there is a transition point from the slab bridge to the prestressed girder bridge.

At a span length of 18 meters, the prestressed girder bridge has the lowest carbon footprint compared to the other two bridge types. Between 18 and 20 meters of the girder bridge, the lowest total CO_2-eq transition to the steel-concrete composite bridge.

From 20 meters to 40 meters of span length, the composite bridge has the lowest ecological footprint compared to the other two bridges for a 12-meter wide carriageway.

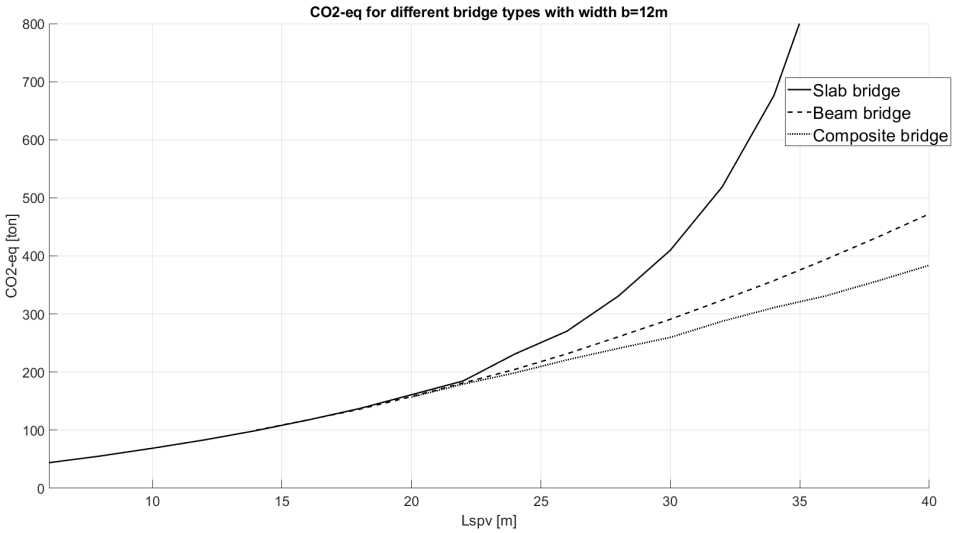

Figure 4.7: *Comparison carriageway width b=12m.*

Table 4.18: Comparison between bridges CO_2-eq, at 12 meter carriageway width.

L_{spv} [m]	Slab bridge CO_2-eq[tons]	Girder bridge CO_2-eq[tons]	Steel-concrete comp. CO_2-eq[tons]
6	**44.0**	-	-
8	**55.6**	-	-
10	**68.9**	-	-
12	**83.2**	-	-
14	**99.3**	99.9	-
16	**117.5**	117.7	-
18	137.3	**136.1**	-
20	161.0	157.8	**157.0**
22	184.8	181.3	**179.3**
24	231.3	204.7	**198.7**
26	270.3	231.4	**221.0**
28	331.2	260.9	**240.9**
30	409.9	291.0	**259.8**
32	518.8	323.9	**287.5**
34	676.2	357.5	**311.0**
36	928.0	394.0	**331.2**
38	-	432.3	**356.9**
40	-	472.4	**384.0**

5
Discussion

5.1 General discussion about the result

The result in Section 4.4 supports the conclusion that there is no bridge type that provides a general lower CO_2-eq emissions for the studied range of span length.

5.2 Simplifications

In this thesis, three different bridge types is investigated and compared their total CO_2-eq emissions from the construction material to find out the bridge type with the lowest emissions for a specific span length and bridge width. When designing bridges there are some limitations that need to be fulfilled but have not been considered in this thesis. The free height is one issue that needs to be considered for many constructions as the needed construction height depends on the site for each project. For the evaluated bridge types in this thesis, mainly the steel-concrete composite bridge has a higher construction height compared to the other two types.

The carbon footprint calculation from Tyréns (Tyrens, 2019) has been developed to determine the amount of climate impact, measured in CO_2-eq, generated by a construction project. This includes the construction, operation, and maintenance of roads and railways. In addition to values expressed in these CO_2-eq from Tyréns, it may be possible to propose additional measures to reduce the climate impact through active choices, such as using 'green' concrete or fossil-free steel. However, further investigations are required to ascertain this, as there are one or more parameters that may come into play. Besides carbon footprint, other factors might influence the decision when selecting a bridge type. Such as costs, advantageous design solutions for specific projects such as construction height of superstructure, accessibility at the construction site, and so on.

In this study, a simplified methodology has been employed, eliminating specific checks and load combinations for all bridge types. This experience-driven approach has resulted in time efficiencies and has played a crucial role in conducting the study in a comprehensive way. It is important to note that the results, along with other assumptions, are solely derived from rough estimations and should be regarded as comparative values rather than definitive figures.

The fatigue verification has only been considered for the steel-concrete compos-

ite bridge, due to the other two bridges do not have any steel components and with experience from Inhouse Tech Göteborg AB the conclusion was made that usually, it is not a critical control in concrete bridges. When fatigue is not critical for one or more details in the I-girder it is allowed to increase the steel grade, the benefit of increasing steel class is that it is possible to reduce the size of the detail, in this thesis the simplification that only steel grade S355 is considered for the steel details.

The fatigue load is depending on the actual traffic situation and is this thesis the assumption that the road is a main road with a low amount of heavy lorries according to (CEN., 2009). The result of the total amount of CO_2-eq for the composite bridge will differ a lot between the chosen road type with the corresponding amount with heavy lorries.

6
Conclusion

In this master's thesis, a tool was developed in MathCAD to optimize three different bridge types regarding the total amount of CO_2-eq emissions and to compare them to find out the bridge type with the lowest emissions for a specific bridge length and carriageway width.

The project indicates that with an active selection of bridge type for a specific bridge length and width, there is an opportunity to reduce the amount of CO_2-eq emissions. With the knowledge gained from the project, the conclusion is that a slab bridge is most optimal regarding emissions for bridges with low span lengths, and for higher span lengths girder bridges and composite bridges are most beneficial.

One conclusion that was made at the higher span lengths was that the carriageway width is important to consider. As the results show, the bridge with 6 meter carriageway width will only the girder bridge be dominant as the bridge with lower CO_2-eq, for the 9 meter carriageway width at the highest span lengths the results shows that the steel-concrete composite bridge will have a lower CO_2-eq total amount. When increasing the width to 12m the same pattern follows and the steel-concrete composite bridge will be dominant as the best bridge regarding CO_2-eq for the higher span lengths.

6.1 Further studies

In this thesis, the calculation of the capacity for each bridge has been simplified and by experience from Inhouse Tech Göteborg AB only the most critical controls have been tested. In further studies, verification with a FEM analysis is recommended to verify the results for each bridge type.

In this study, assumptions regarding the contribution of the foundation CO_2-eq emissions have been assumed to be applicable to all three bridge types. It would be interesting to consider the amount of foundation requirement in further studies, taking into account the bridge's self-weight, in order to determine a specific contribution of CO_2-eq for each bridge type.

In this study, the emission factors for each building material have been obtained from (Tyrens, 2019), which also forms the basis for Trafikverket's carbon calculation. In that report, an average value has been calculated for each building material

to facilitate the implementation of an LCA assessment. It would be interesting to further investigate what happens if one of these values for a material is replaced with a more environmentally friendly alternative, such as green concrete.

References

Al-Emrani, M., & Aygül, M. (2014). *Fatigue design of steel and composite bridges.* CHALMERS UNIVERSITY OF TECHNOLOGY, Göteborg.

Alhede, A., & Beskow, K. (2020). *Parameter study and optimization of slab frame bridges.* Master's thesis: Chalmers University of Technology. Gothenburg.

Bengtsson, A., & Wolf, J. P. (1969). *Strip (structural integrated programs) users manual step-2. plane member systems.* In Swedish: Nordisk ADB AB, Stockholm, in German: Digital AG, Zürich.

Boverket. (2019a). *Mer om miljövarudeklaration för byggprodukter (epd) - boverket.* Retrieved from `https://www.boverket.se/sv/byggande/hallbart-byggande-och-forvaltning/livscykelanalys/miljodata-och-lca-verktyg/miljovarudeklaration-for-byggprodukter-epd/`

Boverket. (2019b). *Vad visar en lca? - boverket.* Retrieved from `https://www.boverket.se/sv/byggande/hallbart-byggande-och-forvaltning/livscykelanalys/vad-visar-en-lca/`

Boverket. (2023). *Mer om miljövarudeklaration för byggprodukter (epd).* Retrieved from `https://www.boverket.se/sv/byggande/hallbart-byggande-och-forvaltning/miljoindikatorer---aktuell-status/`

CEN. (2002a). *Eurocode 0: Basis of structural design.* CEN European Committee for Stardardization. Brussels.

CEN. (2002b). *Eurocode 1: Actions on structures - part 1-1: General actions - densities, self-weight, imposed loads for buildings.* CEN European Committee for Stardardization. Brussels.

CEN. (2003). *Eurocode 1: Actions on structures-part 2: Traffic loads on bridges.* CEN European Committee for Stardardization. Brussels.

CEN. (2005a). *Eurocode 2: Design of concrete structures - part 1-1: General rules and rules for buildings.* CEN European Committee for Stardardization. Brussels.

CEN. (2005b). *Eurocode 2: Design of concrete structures – part 2: Concrete bridges – design and detailing rules.* CEN European Committee for Stardardization. Brussels.

CEN. (2005c). *Eurocode 3: Design of steel structures-part 1-1: General rules and rules for buildings.* CEN European Committee for Stardardization. Brussels.

CEN. (2005d). *Eurocode 3: Design of steel structures-part 1-9: Fatigue.* CEN European Committee for Stardardization. Brussels.

CEN. (2005e). *Eurocode 4: Design of composite steel and concrete structures - part 1-1: General rules and rules for buildings.* CEN European Committee for Stardardization. Brussels.

CEN. (2005f). *Eurocode 4 – design of composite steel and concrete structures – part 2: General rules and rules for bridges.* CEN European Committee for Stardardization. Brussels.

CEN. (2006). *Eurocode 3: Design of steel structures - part 1-5: Plated structural elements.* CEN European Committee for Stardardization. Brussels.

CEN. (2009). *Eurocode 3: Design of steel structures-part 2: Steel bridges.* CEN European Committee for Stardardization. Brussels.

CEN. (2016). *Sis-cen/tr 16949:2016 - road restraint system – pedestrian restraint system – pedestrian parapets.* CEN European Committee for Stardardization. Brussels.

Engström, B. (2007). *Restraint cracking of reinforced concrete structures.*

Engström, B. (2011). *Design and analysis of prestressed concrete structures.* Chalmers university of technology.

Engström, B. (2014). *Design and analysis of slabs and flat slabs.* Chalmers university of technology.

Fossilfritt Sverige. (2018). *Bygg-och anläggningssektorn färdplan för fossilfri konkurrenskraft.*

Jernkontoret. (2018). *Klimatfärdplan : för en fossilfri och konkurrenskraftig stålindustri i sverige.*

Pacoste, C., Plos, M., & Johansson, M. (2012). *Recommendations for finite element analysis for the design of reinforced concrete slabs.* KTH, Stockholm.

PTC. (2023). *Ptc mathcad prime.* Retrieved from `https://www.mathcad.com/`

Statens betongkommité. (1969). *Bestämmelser för betongkonstruktioner, allmänna konstruktionsbestämmelser.* AB Svensk Byggtjänst, Stockholm.

Svensk Betong. (2022). *Vägledning klimatförbättrad betong.*

Svensson, A., & Pålsson, P. R. (2023). *Mathcad calculation softwares for early estimation of bridges with regards to lca. doi:10.5281.* Retrieved from `https://doi.org/10.5281/zenodo.7989624`

Trafikverket. (2008). *Kodförteckning och beskrivning av brotyper.*

Trafikverket. (2019). *Tdok 2016:0204 - krav brobyggande.*

Trafikverket. (2022). *Trvinfra-00227 - bro och broliknande konstruktion, byggande trafikverkets infrastrukturregelverk.*

Transportstyrelsen. (2018). *Tsfs-2018:57 transportstyrelsens föreskrifter och allmänna råd om tillämpning av eurokoder - tsfs.*

Tyrens. (2019). *Klimatkalkyl -uppdatering av emissionsfaktorer.*

Vägverket. (1996). *Broprojektering.* Vägverket Borlänge.